Applied Catalysis B: Environmental 181 (2016) 332–351

Contents lists available at ScienceDirect

Applied Catalysis B: Environmental

journal homepage: www.elsevier.com/locate/apcatb

Review

Copper based catalysts for the selective ammonia oxidation into nitrogen and water vapour—Recent trends and open challenges

Magdalena Jabłońska, Regina Palkovits*

Chair of Heterogeneous Catalysis and Chemical Technology, RWTH Aachen University, Worringerweg 2, 52074 Aachen, Germany

ARTICLE INFO

Article history:
Received 21 March 2015
Received in revised form 7 July 2015
Accepted 13 July 2015
Available online 5 August 2015

Keywords:
Ammonia
Selective catalytic oxidation
NH_3-SCO
NH_3-SCR
Copper
i-SCR mechanism

ABSTRACT

More restrictive standards of Euro VI concerning nitrogen oxide (NO_x = NO, NO_2) emissions necessitate an enhanced urea injection, while generating a higher ammonia slip, which is also precisely limited. For this reason, ammonia slip catalysts (ASC) are an essential part of efficient aftertreatment systems. Currently, supported noble metal catalysts are applied but possess limited selectivity to nitrogen. Copper based catalysts present a promising alternative for the selective catalytic ammonia oxidation into nitrogen and water vapour (NH_3-SCO). This review article focusses on NH_3-SCO as appropriate solution to abate unreacted ammonia particularly after the selective catalytic reduction of NO_x with ammonia (NH_3-SCR, $DeNO_x$). A brief overview of potential catalyst systems is provided, followed by a comprehensive discussion of copper based catalysts. Potential material classes including oxides, exchanged zeolites, modified clays or mixed forms are described systematically. The review focusses on structure-performance correlations covering copper loading, redox properties of CuO species and available acid sites of the catalysts. Another emphasis concerns the influence of the feed composition on the catalytic performance including the content of oxygen and water vapour or sulphur oxide in the feed. Finally, the proposed *i-SCR* mechanism over copper based catalysts, including bimetallic systems, is described and critically reviewed followed by general conclusions together with a discussion of promising research directions.

Contents

* Corresponding author. Fax: +49 241 80 22177.
E-mail address: Palkovits@itmc.rwth-aachen.de (R. Palkovits).

http://dx.doi.org/10.1016/j.apcatb.2015.07.017
0926-3373/

1. Introduction

Ammonia (NH_3) is a colourless, toxic and corrosive gas with an unpleasant pungent odor, emitted by both biogenic and anthropogenic sources [1]. Ammonia and ammonium salts, i.e. phosphates, sulphates or nitrates are potentially harmful to human health and environment [2–6]. Ammonia odor is detected by human nose already at levels of 5–10 ppm. Below 50 ppm, an irritation of the respiratory system, skin and eyes, occurs [7]. Overexposure to ammonia over 300 ppm can cause lung diseases (e.g. bronchitis, bronchopneumonia or fibrosis of the lung tissue with severe respiratory failure) [8], while 500 ppm and above present a serious danger to health and life [9]. Finally, a NH_3 concentration above 10,000 ppm was reported to be lethal within 5–10 min [10]. Amshel et al. [11] summarized potential effects of ammonia on human health in a review. Therefore, it is not surprising to find NH_3 among four main atmospheric pollutants together with nitrogen oxides (NO_x), sulphur oxides (SO_x) and non-methane volatile organic compounds (NMVOC) [12]. Depending on the application, a variety of techniques for the elimination of gaseous ammonia exists. Absorption, adsorption, condensation, biofiltration, catalytic combustion, catalytic decomposition, thermal and selective catalytic oxidation have been applied (e.g. [13–27]). Busca and Pistarino [2] presented a broad summary of the mentioned technologies, their advantages and major drawbacks. Considering the technical and/or economical limitations of treatment technologies of gaseous ammonia, none of them presents a universal solution. In particular, the concentration of ammonia appears to be a main parameter for selection of an appropriate technology.

An efficient current technology, dedicated especially to the treatment of large gas flows containing oxygen and low concentrations of ammonia, is the selective catalytic oxidation into nitrogen and water vapour (e.g. [28–32]). The application areas for NH_3-SCO include for instance the treatment of waste gases from chemical production processes, ammonia slip from the NH_3-SCR process and gasification of biomass (e.g. [33–38]). The desired products of NH_3-SCO are nitrogen and water vapour, while nitrogen oxides (N_2O, NO) are side-products [39]. Different NH_3 oxidation paths can occur dependent on operation conditions and the type of catalyst used (Fig. 1).

2. Ammonia slipstream treatment

As stated above, the selective catalytic oxidation of ammonia into nitrogen and water vapour can be a solution to pollutions caused by various sources of ammonia emissions. NH_3-SCO is applied to abate ammonia slip after the selective catalytic reduction of nitrogen oxides (NO, NO_2) with ammonia (NH_3-SCR) used in power plants as well as after-treatment systems of diesel exhausts (e.g. [40–42]). Currently, the NH_3-SCR process is the most important and well-established process used to abate nitrogen oxides, rapidly and effectively at moderate temperatures, i.e. 250–400 °C, over V_2O_5–TiO_2 oxide with addition of either WO_3 or MoO_3

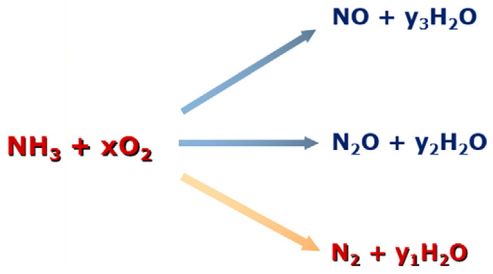

Fig. 1. Principal ways of catalytic oxidation of ammonia.

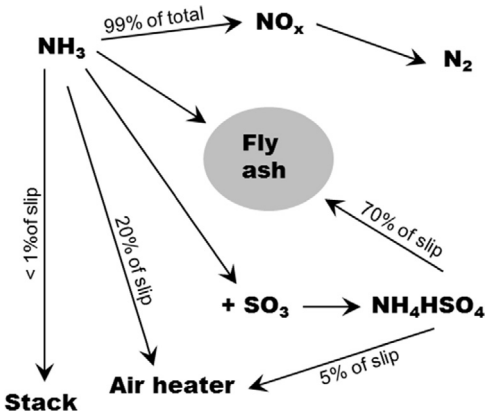

Fig. 2. Fate of ammonia in flue gas. Adapted from Ref. [50], copyright granted by L. Larrimore.

[40,43,44]. A more detailed description of the NH_3-SCR technology is presented in several publications (e.g. [41,43,45]). In a typical NH_3-SCR process, the ratio of NO to NH_3 is 1:1 as represented by Eq. (1):

$$4NO + 4NH_3 + O_2 \rightarrow 4N_2 + 6H_2O \quad (1)$$

The challenge is to achieve high NO conversion, while the main drawback is unreacted ammonia the so called ammonia slip, which results from an incomplete reaction (1). Ammonia emissions are strictly limited to 2–10 ppm as a typical NH_3 slip threshold limit [46,47]. Besides a potential impact on human health, ammonia slip may cause corrosion or plug of downstream equipment due to the formation of ammonium sulphate and/or agglomerated fly ash [46,48]. Of course, effects such as ammonium sulphate formation strongly depend on the specific system design and e.g. SO_3 levels [49]. An example of a proposed ammonia deposition mechanism on coal ash is illustrated in Fig. 2.

To avoid ammonia slip, NH_3-SCR is generally carried out with an under stoichiometric amount of ammonia (NH_3/NO = 0.90–0.95) resulting in a decreased efficiency of NO_x elimination. A strategy for improving the abatement of NO_x emissions is using stoichiometric or even an excess quantity of ammonia and adding a second layer of catalyst able to realize the selective catalytic oxidation of residual ammonia into nitrogen and water vapour (Fig. 3) [42,51]. One major advantage of NH_3-SCO relies on the fact that no addi-

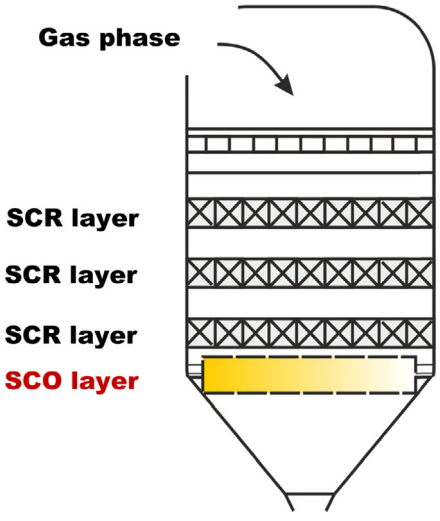

Fig. 3. Industrial SCR reactor. Reprinted from Ref. [52] with permission of OmniScriptum GmbH & Co. KG.

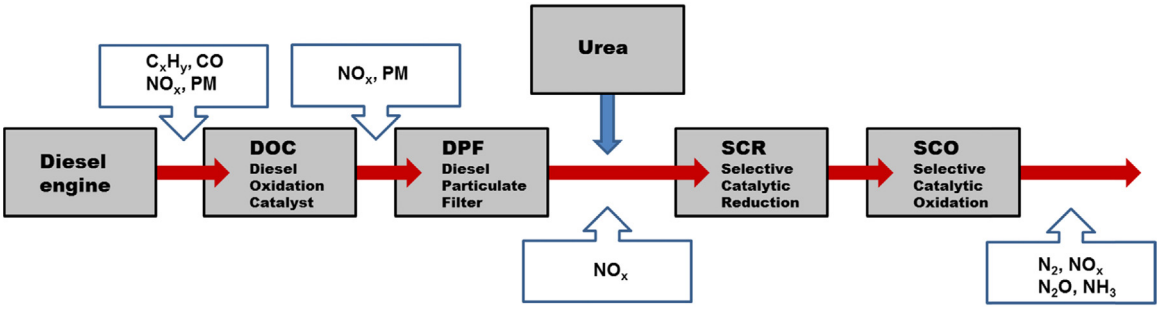

Fig. 4. Diesel aftertreatment system. Adapted from Ref. [58], copyright granted by P. Marsh.

tional reactants are needed since the reaction proceeds between components present in waste gases as shown by Eq. (2):

$$4NH_3 + 3O_2 \rightarrow 2N_2 + 6H_2O \quad (2)$$

So called guard catalysts, ammonia slip catalysts (ASC) or ammonia oxidation catalysts (AMOX) facilitate an overdosing of NH_3 increasing the NO_x conversion in the reduction system [33,53]. However, despite several studies devoted to catalysts for a selective ammonia oxidation, a catalyst possessing high activity and selectivity over the required temperature range has not been presented yet. Major challenges are associated with the design of a suitable downstream catalyst: (i) the catalyst should exhibit high activity at relatively low temperatures (<400 °C) in order to avoid the need for additional heating of exhaust gases, (ii) the material has to possess sufficient stability in the presence of high concentrations of water vapour or other components of waste gases (CO_x, SO_x) and (iii) should selectively convert NH_3 into N_2 [28,36,54]. Additionally, the NH_3-SCR process was originally developed for stationary emission sources, mainly power plants, where the temperature of exhaust gases is relatively low and varies only in a narrow range of 250–400 °C [55,56]. However, it soon turned out to be a promising technology for the NO_x removal in automobile applications [57]. In 2005, NH_3-SCR using an urea solution for on-board NH_3 generation (AdBlue, DEF, in Europe or US, respectively) as the reductant was introduced for commercial heavy-duty vehicles in Europe, and more recently also for passenger cars [58–60]. Different solutions have been applied and patented (e.g. [61–64]). The NH_3-SCR catalyst is often placed downstream of the diesel particulate filter (DPF) in order to meet the requirements of soot particle emissions (Fig. 4). NO_x can be reduced by soot forming N_2 and CO_2, simultaneously [65]. Therefore, temperatures of exhaust gases emitted by automotive diesel engines vary in a broad range and can increase up to 600 °C, in the cycle of diesel particulate filter regeneration. Thus, work should be done to minimize ammonia slip under these conditions.

3. Catalytic systems

As stated above, the selective catalytic oxidation of ammonia into nitrogen and water vapour is a highly promising process to reduce ammonia emissions into the atmosphere. However, depending on the used catalytic system, the catalytic performances can strongly differentiate. Il'chenko [66] published one of the earliest contributions in the area of selective ammonia oxidation. The author compared transition metal oxides at 230 °C and observed decreasing catalytic activity in the following order: MnO_2, Co_3O_4 > CuO > CaO > NiO > Bi_2O_3 > Fe_2O_3 > V_2O_5 > TiO_2 > CdO > PbO > ZnO > SnO_2 > ZrO_2 > MoO_3 > WO_3. A similar order of catalytic activity of transition metal oxides has been presented in another study as well [67]: Co_3O_4 > MnO_2 > Cr_2O_3 > Fe_2O_3 > CuO > NiO > V_2O_5 > MoO_3 > U_3O_8 > ThO_2 > WO_3 > SnO_2 > ZrO_2 > ZnO > Nb_2O_5 > Sb_2O_4 > Ta_2O_5. Interestingly, simple Co_3O_4 and MnO_2 showed high catalytic activity, but the main reaction by-product was N_2O [66]. At higher temperatures, i.e. 720–820 °C, Co_3O_4 was found to be highly selective to NO [68,69]. On the other hand, the oxide most selective for N_2 formation was V_2O_5, with close to 100% N_2 formation at 230 °C, but very low catalytic activity compared to Co_3O_4 [66]. Additionally, at higher temperatures, V_2O_5 mainly facilitated N_2O formation [28]. Therefore, further work was aimed at improving selectivity to N_2 and decreasing temperature of ammonia oxidation. Until now various types of catalysts have been studied for the selective ammonia oxidation into nitrogen and water vapour and were classified into three main groups: (i) (supported) noble metals, such as Ag, Pt, Pd, Ru or Ir (e.g. [53,66,70–81]), (ii) (supported) transition metal oxides including CuO, Fe_3O_4, Co_3O_4, NiO, V_2O_5 (e.g. [32,51,66,82–96]), or (mixed) rare earth oxides like CeO_2 or La_2O_3 and transition metal oxides (e.g. [29,74,76,81,97–102]), (iii) noble (transition) metal-modified zeolites, such as Cu-ZSM-5, Pd-Y, Rh-ZSM-5, Fe-Beta (e.g. [26,28,66,74,83,89,103–112]).

The first generation of ammonia slip catalysts used platinum supported on an appropriate oxide (e.g. [53,79]). Pt/Al_2O_3 was reported as one of the most active catalysts for NH_3-SCO. Unfortunately it caused significant N_2O and NO formation [28,53,79]. High selectivity towards NO_x was also found for other noble metal based catalysts. Additionally, the high costs of noble metals motivated researchers to look for alternative catalytic systems. (Supported) transition metal oxides have been widely studied in the scientific literature (e.g. [66,67,89]). This type of catalysts showed higher selectivity to N_2, however, they need significantly higher operation temperatures as high as 300–500 °C, than noble metal catalysts. For pure rare earth oxides, such as ceria, the catalytic activity was quite poor, with not satisfying selectivity to N_2 [97,100]. Better results were achieved over cerium composite catalysts, but still operating at temperatures above 400 °C is necessary (e.g. [98,100,101]). Concerning zeolites as catalysts for NH_3-SCO, the same challenges occur. Therefore, up to now and to the best of our knowledge no system of sufficient activity, selectivity to N_2 and long-term stability at low temperatures, i.e. <400 °C could be identified. Table 1 summarises the discussed catalyst systems.

In NH_3-SCO, almost 100% conversion of ammonia is required in order to eliminate ammonia odour [116]. Altogether, a design of oxidation catalysts of high efficiency, selectivity to N_2 and stability remains challenging. A promising class of catalysts are Cu based systems which will be discussed more comprehensively in the following.

4. Copper based catalysts

Among mentioned above catalytic systems tested so far in the selective ammonia oxidation into nitrogen and water vapour, especially copper based catalysts found increasingly

Table 1
Examples of literature data related to ammonia oxidation catalysts [52].

Catalyst system	Advantages	Disadvantages	Ref.
(Supported) noble metals	High activity below 350 °C	Low selectivity to N_2 (NO/N_2O formation)	(e.g. [28,53,90,113–115])
(Supported) transition metal oxides	High selectivity to N_2	Low activity at temperatures below 400 °C	(e.g. [51,84,88,103])
(Mixed) rare earth and transition metal oxides	High selectivity to N_2	Low activity below 400 °C	(e.g. [98,100,101])
Transition metal-modified zeolites	High selectivity to N_2	Low activity below 400 °C	(e.g. [28,83,109,105])
Noble metal-modified zeolites	High activity below 350 °C	Low selectivity to N_2 (NO/N_2O formation)	(e.g. [28,105])

attention including: (i) polycrystalline copper (e.g. [113,117]), (ii) (supported) copper oxides (e.g. [76,86,87,107,118–120]), (iii) (mesoporous) spinels (e.g. [121]) (iv) copper exchanged zeolites (e.g. [90,103,105,107,118]) or (v) modified clays (e.g. [122–125]) as well as (vi) mixed compositions (e.g. [33,126]). We summarized the catalytic performances of these catalysts (Table 2) as well as their physicochemical properties (Table 3). All presented catalysts are able to oxidize ammonia into N_2. However, their optimum operation window for high activity, selectivity and stability unfortunately mostly differs from the region required for a technical application. The following sections allow a more detailed view on individual copper based catalyst systems.

4.1. Copper oxides

In the order of Il'chenko [66], copper oxide was found as one of the most efficient catalysts in selective ammonia oxidation into nitrogen and water vapour. Further studies over preoxidised polycrystalline copper foil proved copper oxide as active phase for NH_3-SCO [113,117]. However, due to unsatisfying selectivity to N_2, further studies concerning ammonia oxidation over copper oxide supported e.g. on γ-Al_2O_3 (e.g. [53,90,127–129]) or TiO_2 (anatase) (e.g. [89,120,130]) were carried out.

Gang et al. [90,103] studied Cu/Al_2O_3 catalysts with different content of copper, i.e. 5.0–15.0 wt.%. Complete oxidation of NH_3 for catalysts with 10.0 wt.% of copper loading occurred at about 350 °C with 90% selectivity to N_2 and a productivity of around 2.85×10^{-6} mol(N_2) s^{-1} g^{-1}. Similar results were obtained by other researchers working with catalysts possessing 10.0 wt.% of copper loading and prepared at similar calcination temperatures (500, 600 °C) [75,128,131]. A significantly higher productivity with value of 8.19×10^{-6} mol(N_2) s^{-1} g^{-1} was achieved over (3.4 wt.%)Cu/Al_2O_3 by applying low catalyst loadings, i.e. 25 mg [107,118].

A further increase of the copper loading did not significantly influence the catalytic performance of these catalysts [90,103], while higher calcination temperatures of 700–900 °C resulted in a significant decrease of the catalytic performance [36,119,127]. Besides copper loading and calcination temperature, precursor selection and preparation method were reported to influence the final copper oxide species. For example, a sulphate precursor led to the formation of $CuAl_2O_4$, while CuO of higher crystallinity was formed using an acetate compared to a nitrate precursor [131]. However, the nature of the active species in NH_3-SCO has not been fully clarified yet. Gang et al. [90,103] claimed that a $CuAl_2O_4$-like surface phase is responsible for higher catalytic activity compared to CuO. A comprehensive study conducted by Liang et al. [131] confirmed that a mixture of both CuO and $CuAl_2O_4$ had significant influence on the Cu/Al_2O_3 catalyst performance. Catalysts containing easily reducible CuO species presented not only superior catalytic activity at lower temperatures, but possessed a significant decrease of N_2 selectivity above 250 °C. On the other hand, not only reducibility of the CuO species, but also particle size influences the catalytic performance of the catalysts. Lippits et al. [29] used different preparation method, i.e. homogeneous deposition precipitation followed by reduction instead of impregnation and calcination in air, and produced small metallic particles with an average size of 3.6 nm at low Cu loadings. These metallic particles were readily oxidized to copper oxide under an oxygen rich reaction environment (NH_3:O_2 = 1:5–25). Interestingly, this (1.3 wt.%)Cu/Al_2O_3 catalyst exhibited superior activity with regard to the copper content and higher selectivity to N_2 together with higher productivity in comparison to (10.0 wt.%)Cu/Al_2O_3 presented by Gang et al. [90,103] (Table 2, pos. 2 and pos. 9). Lin et al. [76] compared the catalytic performance over calcined or H_2-pretreated (8.7 wt.%)Cu/Al_2O_3 catalysts and confirmed superior activity of the calcined catalysts but only in the low temperature range. Note, that the feed composition was 1:1 (NH_3:O_2). Therefore, a possible explanation of lower activity could be incomplete copper oxidation of the pretreated catalyst. On the other hand, N_2 selectivity was not significantly affected by the preparation technique.

Comparing 10.0 wt.% Cu supported on Al_2O_3 or TiO_2 as support materials demonstrated a similar selectivity to N_2 and productivity but significantly higher catalytic activity of Cu/TiO_2 for NH_3-SCO [120]. The authors concluded TiO_2 (anatase) to be more suitable as support than γ-Al_2O_3 due to its higher oxygen mobility and lower oxygen bonding strength. In line, also several studies on the selective catalytic reduction of NO_x (NH_3-SCR) utilized titania as support material (e.g. [132–134]). Further, investigations focusing on ammonia oxidation conducted by Wöllner et al. [86] revealed complete ammonia conversion over bimetallic, copper and manganese oxides supported on TiO_2 (anatase) for temperatures above 300 °C. It was found that the most active catalyst with a Cu:Mn molar ratio of 20:80 contained a nonstoichiometric $Cu_{1.4}Mn_{1.6}O_4$ crystalline spinel phase and Mn_2O_3 mainly in the amorphous phase, respectively. Unfortunately, the N_2 selectivity of these materials was not clearly reported.

A similar concept for manganese promotion of a mixture of copper chromites, i.e. $CuO/CuCr_2O_4$ and $CuCrO_2$ was suggested by Kaddouri et al. [135]. However, the catalytic performance of manganese doped catalyst, in ammonia oxidation was almost the same as that reported over $CuO/CuCr_2O_4$ and $CuCrO_2$ above 240 °C. Moreover, in both cases the selectivity to N_2 and productivity were low, while the presence of chromium compounds may additionally be harmful for human health and environment (e.g. [136,137]).

An application of other spinels for NH_3-SCO was further investigated by Yue et al. [121]. Interestingly, they compared a mesoporous $CuFe_2O_4$ with conventional materials prepared by hard-templating and sol–gel synthesis, respectively. Mesoporous $CuFe_2O_4$ exhibited superior catalytic activity and selectivity to N_2, which was mainly assigned to the higher specific surface area of the material associated with a larger number of accessible acidic surface sites as well as higher reducibility of CuO species. Higher specific surface area of catalyst allowed more copper oxides species to be exposed to the reducing atmosphere. In comparison to Cu/Al_2O_3 (e.g. [90,103]), the mesoporous spinel possessed similar catalytic performance, however, its preparation is more sophisticated. Cui et al. [138] used a hard-templating approach in order to synthesize mesoporous CuO/RuO_2. The temperature for complete ammonia oxidation over those materials was as low as 180 °C with a selectivity to N_2 over 95% on the mesoporous (10.0 wt.%)CuO/RuO_2 catalyst. Further increasing the copper loading did not improve the

Table 2
Review of catalytic performances of copper based catalysts for selective ammonia oxidation into nitrogen and water vapour (NH_3-SCO).

Pos.	Catalyst code	T (°C)	NH_3 conversion (%)	N_2 selectivity (%)	Productivity** (10^{-6} mol s^{-1} g^{-1})	Ref.
1	Cu (polycrystalline, O_2-oxid.)	397	20	90	*	[113]
2	Cu/Al_2O_3 (400 °C, H_2-red.)					[29]
	(1.3 wt.% Cu)	350	100	98	5.83	
3	Cu/Al_2O_3 (450 °C, air-calc.)					[107,118]
	(3.4 wt.% Cu)	400	100	51	8.19	
4	Cu/Al_2O_3 (300 °C, H_2-red.)	300	72	98	2.1	[76]
	Cu/Al_2O_3 (500 °C, O_2-oxid.)		64	98	1.87	
	(8.7 wt.% Cu)					
5	Cu/Al_2O_3 (450 °C, air-calc.)					[120]
	(10.0 wt.% Cu)	400	100	95	0.71	
6	Cu/Al_2O_3 (500 °C, air-calc.)					[75]
	(10.0 wt.% Cu)	350	100	90	2.85	
7	Cu/Al_2O_3 (600 °C, air-calc.)					[131]
	(10.0 wt.% Cu)	350	100	93	0.35	
8	Cu/Al_2O_3 (600 °C, air-calc.)					[128]
	(10.0 wt.% Cu)	350	90	95	3.18	
9	Cu/Al_2O_3 (600 °C, air-calc.)					[90,103]
	(5.0 wt.% Cu)	350	75	96	2.28	
	(10.0 wt.% Cu)		100	90	2.85	
	(15.0 wt.% Cu)		100	94	2.98	
10	Cu/Al_2O_3 (700 °C, air-calc.)					[36,127]
	(10.0 wt.% Cu)	700	40	–	*	
11	Cu/Al_2O_3 (900 °C, air-calc.)					
	(10.0 wt.% Cu)	900	27	–	*	
12	Cu/Al_2O_3 (800 °C, air-calc.)					[119]
	(20.0 wt.% Cu)	400	81	–	*	
13	Cu/TiO_2 (450 °C, air-calc.)					[120]
	(10.0 wt.% Cu)	250	100	95	0.71	
	(20.0 wt.% Cu)		100	92	0.68	
14	$Cu/Mn/TiO_2$ (550 °C, air-calc.)					[86]
	(100.0 mol% Cu)	300	85	–	*	
	(40.0 mol% Cu)		97	–	*	
	(20.0 mol% Cu)		99	–	*	
15	$Au/Cu/Al_2O_3$ (300 °C, H_2-red.)					[76]
	(3.0 wt.% Au/1.0 mol% Cu)	327	100	95	2.83	
	(4.6 wt.% Au/1.0 mol% Cu)		100	88	2.62	
	(5.0 wt.% Au/1.0 mol% Cu)		100	95	2.83	
16	$Ag/Cu/Al_2O_3$ (500 °C, air-calc.)					[75]
	(7.5 wt.% Ag/2.5 wt.% Cu)	300	100	95	0.35	
17	$Ag/Cu/Al_2O_3$ (600 °C, air-calc.)					[128]
	(5.0 wt.% Ag/5.0 wt.% Cu)	325	100	95	3.53	
	(10.0 wt.% Ag/10.0 wt.% Cu)	275	100	78	2.9	
18	$Pt/Cu/Al_2O_3$ (450 °C, air-calc.)					[70]
	(1.0 wt.% Pt/20.0 wt.% Cu)	210	100	88	1.39	
	(4.0 wt.% Pt/20.0 wt.% Cu)	200	100	82	1.29	
19	$Pt/Cu/Al_2O_3$ (800 °C, air-calc.)					[119]
	(1.0 wt.% Pt/20.0 wt.% Cu)	350	60	–	*	
20	CuCr (450 °C, N_2-calc.)					[135]
	(32.6 wt.% Cu)	243	95	32	0.12	
	Mn/CuCr (450 °C, N_2-calc.)					
	(30.9 wt.% Cu)	248	95	30	0.12	
	(29.6 wt.% Cu)	243	95	27	0.1	
	Ag-Mn/CuCr (450 °C, N_2-calc.)					
	(28.0 wt.% Cu)	238	95	42	0.16	
21	$CuFe_2O_4$ (600 °C, air-calc.)					[121]
	(-wt.% Cu)	400	65	95	0.23	
	$CuFe_2O_4$ (mesoporous, 600 °C, air-calc.)					
	(-wt.% Cu)	350	100	98	0.36	
22	CuO/RuO_2 (mesoporous, 500 °C, air-calc.)					[138]
	(5.0 wt.% CuO)	180	100	95	0.88	
	(10.0 wt.% CuO)		100	97	0.9	

Table 2 (*Continued*)

Pos.	Catalyst code	T (°C)	NH_3 conversion (%)	N_2 selectivity (%)	Productivity** (10^{-6} mol s^{-1} g^{-1})	Ref.
	(15.0 wt.% CuO)		100	97	0.9	
	(20.0 wt.% CuO)	210	100	98	0.91	
	(30.0 wt.% CuO)		100	99	0.92	
23	CuO-CeO_2 (500 °C, air-calc.)					[97]
	(6.0 wt.% CuO)	280	100	90	0.67	
	(8.0 wt.% CuO)	270	100	90	0.67	
	(10.0 wt.% CuO)	250	100	97	0.72	
	(12.0 wt.% CuO)	270	100	92	0.68	
24	CuO/CNTs (350 °C, He-calc.)					[142]
	(9.91 wt.% Cu)	230	100	94	0.7	
	(9.84 wt.% Cu)	220	100	95	0.71	
	(9.88 wt.% Cu)	210	100	97	0.72	
	(9.85 wt.% Cu)	189	100	99	0.74	
25	Cu/Y (400 °C, air-calc.)					[90,103]
	(3.7 wt.% Cu)	300	54	98	1.67	
	(8.4 wt.% Cu)		88	97	2.7	
	(3.7 wt.% Cu, NaOH treatment)		100	98	3.1	
	(8.4 wt.% Cu, NaOH treatment)		100	98	3.1	
26	Cu/Beta (450 °C, air-calc.)					[107]
	(1.2 wt.% Cu)	400	90	98	14.18	
	(3.0 wt.% Cu)	350	100	96	15.43	[118]
	(6.6 wt.% Cu)	300	100	96	15.43	
27	Cu/ZSM-5 (500 °C, air-calc.)					[105]
	(4.4 wt.% Cu)	450	97	100	3.61	
28	PILC-Verm-Cu (500/450 °C, air-calc.)					[124]
	(1.0 wt.% Cu, pillared vermiculite)	500	100	95	1.41	
	PILC-Phlog-Cu (500/450 °C, air-calc.)					
	(1.3 wt.% Cu, pillared phlogopite)	550	90	92	1.23	
29	PCH-Cu (550/450 °C, air-calc.)					[125]
	(0.59 wt.% Cu, porous clay heterostructures)	500	100	99	1.47	
	PCH-NH_3-Cu (550/450 °C, air-calc.)					
	(1.4 wt.% Cu, porous clay heterostructures)	400	100	95	1.41	
30	MgCuAlO*x* (600 °C, air-calc.)					[144]
	(5.0 mol% Cu)	400	100	87	1.29	
	(10.0 mol% Cu)	450	100	64	0.95	
	(20.0 mol% Cu) (hydrotalcite originated mixed metal oxides)	450	100	60	0.89	
31	MgCuCoAlO*x* (600 °C, air-calc.)					[144]
	(5.0 mol% Cu)	450	100	81	1.21	
	(10.0 mol% Cu)	500	100	59	0.88	
	(20.0 mol% Cu) (hydrotalcite originated mixed metal oxides)	500	100	48	0.71	
32	$MgCuFeO_x$ (600 °C, air-calc.)					[122]
	(1.0 mol% Cu)	425	100	78	1.16	
	(0.75 mol% Cu)	425	100	80	1.19	
	(0.5 mol% Cu)	400	100	88	1.31	
	(0.25 mol% Cu) (hydrotalcite originated mixed metal oxides)	425	100	80	1.19	
33	$MgCuAlO_x$ (650 °C, air-calc.)					[146]
	(4.6 mol% Cu)	450	100	–	*	
	(7.2 mol% Cu) (hydrotalcite originated mixed metal oxides)	425	100	–	*	
34	$MgCuAlO_x$ (600 °C, air-calc.)	375	100	90	1.34	[147]
	$MgCuFeO_x$ (600 °C, air-calc.)	400	100	87	1.29	
	$MgCuAlO_x$ (900 °C, air-calc.)	500	100	42	0.63	
	$MgCuFeO_x$ (900 °C, air-calc.) (0.6 mol% Cu hydrotalcite originated mixed metal oxides)	500	100	57	0.85	
35	$MgCuAlO_x$ (600 °C, air-calc.)	437	100	94	1.4	[123]
	Pt/$MgCuAlO_x$ (600/500 °C, air-calc.)	366	100	86	1.28	
	Pd/$MgCuAlO_x$ (600/500 °C, air-calc.)	413	100	76	1.13	
	Rh/$MgCuAlO_x$ (600/500 °C, air-calc.)	415	100	93	1.38	
	(0.05 mol% Pt, 0.1 mol% Pd, Rh, 5.0 mol% Cu hydrotalcite originated mixed metal oxides)					
36	Pt/Al_2O_3-Cu/ZSM-5 (500/500 °C, air-calc.; 650 °C, O_2/Ar-oxid.)					[33]
	(0.46 wt.% Pt/0.8 wt.% Cu)	250	100	58	*	
	(0.46 wt.% Pt/1.6 wt.% Cu)		100	60	*	
	(0.46 wt.% Pt/2.5 wt.% Cu)		100	82	*	
37	Pt/Al_2O_3-Cu/CHA (450–600/450 °C, air-calc.)					[126]
	(0.58 wt.% Pt/2.3 wt.% Cu)	250	91	67	*	

– not shown.
* not calculated.
** Calculated based on provided flow rates, NH_3 conversion and N_2 selectivity not considering volume change.

Table 3
Review of specific surface area (S_{BET}), crystalline phases (XRD), peak temperature of various copper oxide species (H_2-TPR) of different copper based catalysts.

Pos.	Catalyst code	S_{BET} ($m^2\ g^{-1}$)	Crystalline phases	Peak temperature (°C)	Ref.
1	Cu/Al_2O_3 (450 °C, air-calc.)				[118]
	(3.4 wt.% Cu)	–	–	216	
2	Cu/Al_2O_3 (450 °C, air-calc.)				[120]
	(10.0 wt.% Cu)	172	γ-Al_2O_3	–	
3	Cu/Al_2O_3 (600 °C, air-calc.)				[131]
	(10.0 wt.% Cu)	–	CuO, γ-Al_2O_3	305, 335	
4	Cu/Al_2O_3 (600 °C, air-calc.)				[128]
	(10 wt.% Cu)	224	γ-Al_2O_3	–	
5	Cu/Al_2O_3 (700 °C, air-calc.)				[36]
	(10.0 wt.% Cu)	95	CuO, γ-Al_2O_3	–	
6	Cu/Al_2O_3 (900 °C, air-calc.)				
	(10 wt.% Cu)	47	$CuAl_2O_4$, γ-Al_2O_3	–	
7	Cu/Al_2O_3 (800 °C, air-calc.)				[119]
	(20.0 wt.% Cu)	97	CuO, γ-Al_2O_3	–	
8	Cu/TiO_2 (450 °C, air-calc.)				[120]
	(10.0 wt.% Cu)	123	CuO, TiO_2 (anatase)	–	
	(20.0 wt.% Cu)	83	CuO, TiO_2 (anatase)	–	
9	Cu/TiO_2 (550 °C, air-calc.)				[86]
	(100.0 mol% Cu)	32	CuO, TiO_2 (anatase)	207	
	(40.0 mol% Cu)	42		259	
	(20.0 mol% Cu)	47	CuO, $Cu_{1.4}Mn_{1.6}O_4$ Mn_2O_3, TiO_2 (anatase)	244	
10	$Ag/Cu/Al_2O_3$ (600 °C, air-calc.)				[128]
	(5.0 wt.% Ag/5.0 wt.% Cu)	193	γ-Al_2O_3	–	
	(10.0 wt.% Ag/10.0 wt.% Cu)	158	Ag_2O, γ-Al_2O_3	–	
11	$Au/Cu/Al_2O_3$ (350/300 °C, air-calc.)				[76]
	(3.0 wt.% Au/1.0 mol% Cu)	–	γ-Al_2O_3	–	
	(4.6 wt.% Au/1.0 mol% Cu)	–	γ-Al_2O_3	–	
	(5.0 wt.% Au/1.0 mol% Cu)	212	Au, CuO, γ-Al_2O_3	–	
12	$Pt/Cu/Al_2O_3$ (450 °C, air-calc.)				[70]
	(1.0 wt.% Pt/20.0 wt.% Cu)	94	CuO, γ-Al_2O_3	210	
	(4.0 wt.% Pt/20.0 wt.% Cu)	99	CuO, γ-Al_2O_3	160	
13	$Pt/Cu/Al_2O_3$ (800 °C, air-calc.)				[119]
	(1.0 wt.% Pt/20.0 wt.% Cu)	78	Pt, CuO, γ-Al_2O_3	–	
14	CuCr (450 °C, N_2-calc.)				[135]
	(32.6 wt.% Cu)	248	CuO, $CuCr_2O_4$, $CuCrO_2$	–	
	Mn/CuCr (450 °C, N_2-calc.)				
	(30.9 wt.% Cu)	248	CuO, $CuCr_2O_4$, $CuCrO_2$	–	
	Ag/CuCr (450 °C, N_2-calc.)				
	(29.6 wt.% Cu)	220	–	–	
	Ag-Mn/CuCr (450 °C, N_2-calc.)				
	(28.0 wt.% Cu)	16	Ag, Ag_2O, AgO, CuO $CuCr2O_4$, $CuCrO_2$	–	
15	$CuFe_2O_4$ (600 °C, air-calc.)				[121]
	(-wt.% Cu)	12	$CuFe_2O_4$	334	
	$CuFe_2O_4$ (mesoporous, 600 °C, air-calc.)				
	(-wt.% Cu)	194	$CuFe_2O_4$	269	
16	CuO/RuO_2 (mesoporous, 500 °C, air-calc.)				[138]
	(5.0 wt.% CuO)	95	RuO_2	–	
	(10.0 wt.% CuO)	98	CuO, RuO_2	–	
	(15.0 wt.% CuO)	97		–	
	(20.0 wt.% CuO)	103		–	
	(30.0 wt.% CuO)	98		–	
17	CuO–CeO_2 (500 °C, air-calc.)				[97]
	(6.0 wt.% CuO)	145	CeO_2	178, 227	
	(8.0 wt.% CuO)	148		188, 229	
	(10.0 wt.% CuO)	147		192, 229	
	(12.0 wt.% CuO)	131		193, 229	
18	CuO–CeO_2 (500 °C, air-calc.)				[101]
	(6.0 mol% Cu)	61	CuO, CeO_2	–	
19	CuO/La_2O_3 (500 °C, air-calc.)				[98]

Table 3 (*Continued*)

Pos.	Catalyst code	S_{BET} ($m^2\ g^{-1}$)	Crystalline phases	Peak temperature (°C)	Ref.
	(8.0 mol% Cu)	72	CuO, La_2O_3 $La(OH)_3$	–	
20	CuO/CNTs (350 °C, He-calc.)				[142]
	(9.91 wt.% Cu)	–	–	230	
	(9.84 wt.% Cu)	–	–	216	
	(9.88 wt.% Cu)	–	–	208	
	(9.85 wt.% Cu)	–	–	199	
21	Cu/Beta (450 °C, air-calc.)				[118]
	(3.0 wt.% Cu)	–	–	234, 297	
	(3.0 wt.% Cu, after wet testing)	–	–	243, 309	
22	$MgCuFeO_x$ (600 °C, air-calc.)				[122]
	(0.5 mol% Cu)	50	MgO, CuO, Cu_2O, $MgFe_2O_4$ Fe_3O_4, $CuFe_2O_4$	190, 204	
23	$MgCuAlO_x$ (600 °C, air-calc.)	125	MgO	223	[147]
	$MgCuFeO_x$ (600 °C, air-calc.)	42	MgO, CuO, g-Fe_2O_3 $MgFe_2O_4$, $CuFe_2O_4$ Fe_3O_4	205, 227	
	$MgCuAlO_x$ (900 °C, air-calc.)	18	MgO, CuO, Cu_2MgO_3 $(Cu,Mg)Al_2O_4$	223, 252	
	$MgCuFeO_x$ (900 °C, air-calc.)	2	MgO, CuO, g-Fe_2O_3, $MgFe_2O_4$ $CuFe_2O_4$ Cu_2MgO_3, Fe_3O_4	270, 340	
	(0.6 mol% Cu)				
24	$MgCuAlO_x$ (600 °C, air-calc.)				[144]
	(5.0 mol% Cu)	136	MgO	264	
	(10.0 mol% Cu)	130		251	
	(20.0 mol% Cu)	128	–	236	
25	$MgCuAlO_x$ (600 °C, air-calc.)	132	MgO	290	[123]
	$Pt/MgCuAlO_x$ (600/500 °C, air-calc.)	130		260	
	$Pd/MgCuAlO_x$ (600/500 °C, air-calc.)	131		260	
	$Rh/MgCuAlO_x$ (600/500 °C, air-calc.) (0.05 mol% Pt, 0.1 mol% Pd, Rh, 5.0 mol% Cu)	130		255	

– not shown.

catalytic activity, while selectivity to N_2 slightly increased, possibly due to more aggregated CuO species. The presented mesoporous CuO/RuO_2 materials can be considered as one of the most promising candidates for NH_3-SCO. However, note that these catalysts are relatively expensive, hampering their commercialization.

Accordingly, the development of novel and cheaper copper based catalysts is a critical point for NH_3-SCO. In this line, $CuO–CeO_2$ mixed metal oxides have been selected and applied in ammonia oxidation [97,101,139], mainly due to the high efficiency of cerium based materials in various other environmental catalytic processes, such as NO reduction (e.g. [140]), CO oxidation (e.g. [141]) and so forth. In a comprehensive study of Wang et al. [97], $CuO–CeO_2$ catalysts have been compared with regard to the influence of different preparation methods, copper loading and calcination temperatures. All catalysts prepared by a surfactant-templating method and calcined at 500 °C achieved total ammonia oxidation with a selectivity to N_2 over 90% below 300 °C, with the best catalytic performance over a (10.0 wt.%)$CuO–CeO_2$ sample. For this catalyst the highest molar ratio of finely dispersed CuO species, a smaller particle size of CeO_2 of 5.1 nm together with strong synergetic interaction between CuO and CeO_2 were found to be favourable for high activity in NH_3-SCO. Along this line, Song and Jiang [142] studied CuO nanoparticles with an average size of 7–8 nm homogenously dispersed on the surface of carbon nanotubes (CNTs). They emphasised that surface defects of CNTs promote the electron transfer in the reduction process, which destabilizes Cu–O bonds and thus facilitates the reduction of CuO to metallic copper. Consequently, these (9.84–9.91 wt.%)CuO/CNT catalysts oxidized ammonia at a relatively low temperatures (<250 °C) with a N_2 selectivity of above 94%.

In general, the discussed examples confirm high catalytic activity and selectivity for supported copper oxides with a copper loading of around 10.0 wt.% and calcined at relatively low temperatures, i.e. 350–600 °C. The origin of high activity appears to be associated with a high dispersion and easily reducibility of CuO species. Consequently, the preparation procedure and support materials play a crucial role in the design of suitable catalyst systems for NH_3-SCO.

4.2. Copper exchanged zeolites

Since the work of Williamson et al. [143] many studies on copper exchanged zeolites for the selective ammonia oxidation into nitrogen and water vapour have been reported. Il'chenko [66] studied various transition metal exchanged zeolites Y revealing Cu/Y as the most active catalyst for NH_3-SCO. Accordingly, the activity of modified zeolite Y decreased in the following order: Cu > Cr > Ag > Co > Fe > Ni ~ Mn. In all cases, the selectivity to N_2 was above 95%, except for Ag/Y and Cr/Y. Further studies by Gang et al. [90,103] revealed that the catalytic performance of Cu/Y strongly depends on the copper loading as well as alkaline treatment. The activity of the catalysts increased up to 34% increasing the copper loading from 3.7 to 8.7 wt.%. An additional NaOH treatment even caused a further increase of the activity. However, after such treatment both (3.7 or 8.7 wt.%)Cu/Y revealed similar catalytic performance in ammonia oxidation. The significantly dif-

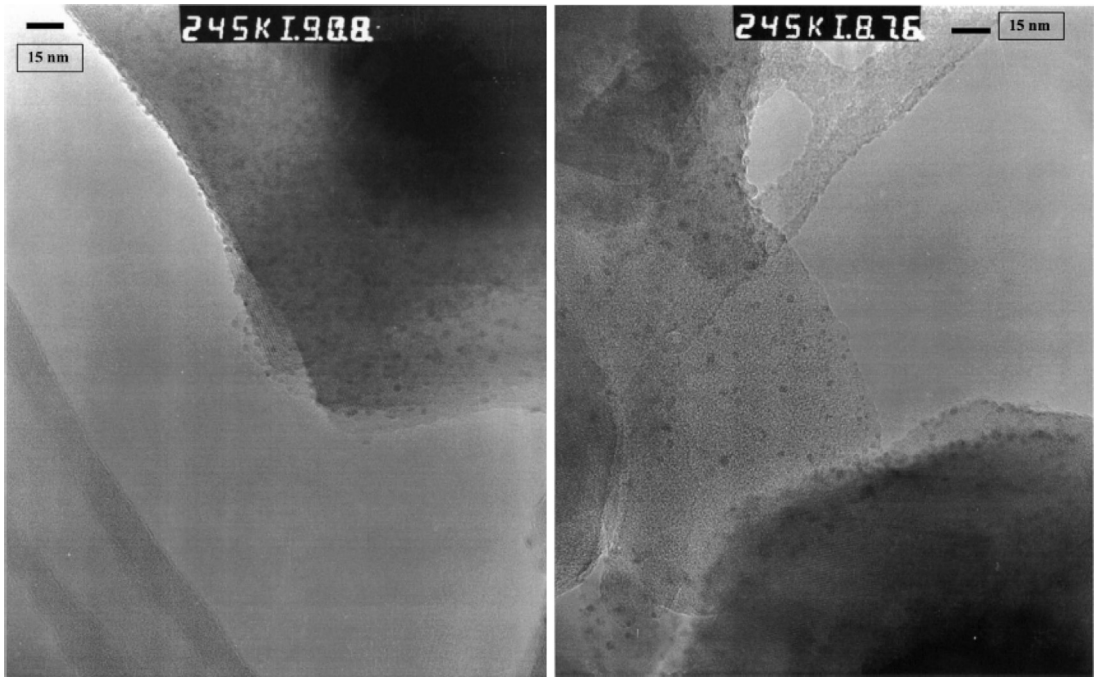

Fig. 5. High-resolution electron microscopy (HREM) images of the (8.4 wt.%)Cu/Y before (left) and after (right) NaOH treatment. Reprinted from Ref. [103] with permission of Elsevier.

ference for different Cu loadings was explained by a change in particle size and dispersion of the copper oxide on the support [90]. However, the influence of NaOH treatment on these factors was not fully clarified hampering a throughout evaluation of the observed differences in activity (Fig. 5) [103]. Nevertheless, these findings are in agreement with the discussed reports on superior catalytic performance in NH_3-SCO over highly dispersed copper particles [29]. Besides copper exchanged zeolite Y, other zeolites, such as ZSM-5 and Beta were tested as potential catalysts for the oxidation of ammonia and showed promising results (e.g. [89,105,107]). Long and Yang [105] studied the catalytic activity of ZSM-5 modified with transition metals. They found the following trend: Fe > Cu > Cr > Pd > H-ZSM-5 > Mn > Ni ~ Co. Complete ammonia conversion was obtained above 450 °C with 100% selectivity to N_2 over (4.4 wt.%)Cu/ZSM-5. Especially copper exchanged zeolite Beta possesses a promising catalytic performance and productivity (e.g. [89,107,118]). The larger pore opening of zeolite Beta in comparison to ZSM-5 could enhance transport of the reactants to the active surface sites and thereby facilitated ammonia oxidation. In fact, (3.0 wt.%)Cu/Beta achieved full ammonia conversion at 350 °C with 96% selectivity to N_2 [107,118]. Further increasing the copper loading to 6.6 wt.% resulted in high activity of the catalyst even at 400 °C with satisfying selectivity to N_2. The most promising feature was the low level of NO and N_2O formed.

In summary, copper exchanged zeolites are a promising class of NH_3-SCO catalysts. However, a full characterisation of copper oxide species present in these materials under reaction conditions has not been attempted yet.

4.3. Copper modified clays

Copper modified vermiculite, phlogopite, porous clay heterostructures and hydrotalcite originated mixed metal oxides present an alternative class of potential catalytic materials for selective ammonia oxidation into nitrogen and water vapour, studied mainly by Chmielarz et al. (e.g. [123–125]). Alumina pillared vermiculite and phlogopite modified with copper proved to be active and selective catalysts of ammonia oxidation [124]. Despite comparable copper loadings for both materials, higher activity could be achieved with vermiculites. The superior activity of vermiculites appears to be caused by more easily reducible CuO species. Additionally, vermiculite was modified facilitating efficient pillaring which causes a higher surface density of acid sites than for phlogopite. In line, alumina pillared vermiculites adsorbed significantly larger quantities of ammonia under reaction conditions resulting in better catalytic activity. Unfortunately, for both materials only low catalytic activity at temperatures below 400 °C could be observed. Above 450 °C also copper modified porous clay heterostructures (PCHs) enabled reasonable catalytic activity [125]. Ammonia treated (1.4 wt.%)Cu-PCH required slightly lower temperatures but still 400 °C for total ammonia conversion. Dinitrogen was the dominating product in the studied temperature range of 300–550 °C.

Hydrotalcite-like compounds were identified as interesting precursors of catalysts for NH_3-SCO (e.g. [122,123,144]). Chmielarz et al. [144] gave an order of activity of transition metals: Cu > Co > Ni > Fe, while the opposite order (with the exception of copper) was observed for the N_2 selectivity. With regard to the optimum copper content in $MgAlO_x$, (5.0 mol%)$CuMgAlO_x$ showed the highest catalytic activity with full ammonia conversion at 400 °C with around 90% N_2 selectivity and a productivity of about 1.29×10^{-6} mol(N_2) s^{-1} g^{-1}. Higher copper loadings of 10.0 or 20.0 mol% did not improve the catalytic performance further. Similar conclusions can be drawn for copper–cobalt systems, though these materials exhibit an overall lower activity compared to $CuMgAlO_x$. Additionally, cobalt raises the point of materials toxicity (e.g. [145]). However, further studies emphasised also copper–iron based materials as promising catalyst candidates [122]. Materials with a molar ratio of copper varying from 0.0 to 1.0 mol% at a constant iron content (e.g. 1.0 mol%) were investigated in NH_3-SCO. A combination of iron in mixed metal oxides together with copper was attempted to achieve higher catalytic performance over a broader temperature range compared to the individual catalysts. The Cu-based catalysts were particularly effective at lower temperatures but less selective to N_2 at higher temperatures. On the other hand, the Fe-based catalysts were active only at higher

temperatures with high selectivity to N_2. Interestingly, a certain copper content is necessary to obtain catalysts active in low temperature ammonia oxidation, while N_2 selectivity decreases with increasing copper loading. A similar trend was also reported by Trombetta et al. [146], as well as for mixed metal oxides prepared at higher calcination temperature, i.e. 900 compared to 600 °C [147]. Focussing on the influence of the calcination temperature, for Mg(Zn)CuAl(Fe)O_x lower calcination temperatures resulted in more active and selective materials. In particular, $MgCuFeO_x$ obtained by calcination at 600 °C allowed full conversion of ammonia at 400 °C, while temperatures around 100 °C higher were necessary for materials calcined at 900 °C. Additionally, a significant drop in selectivity to N_2 from 87 to 57% occurred. This effect was assigned to a significantly lower specific surface area of the catalyst calcined at 900 °C of 2 compared to 42 $m^2\,g^{-1}$ as well as the formation of less reducible more aggregated CuO species.

The catalytic performance of other tested materials proved to be mainly dependent on the presence of copper phases (oxides, spinels) and their redox properties. The catalysts containing easily reduced CuO species presented superior catalytic activity at lower temperatures together with a significant decrease in selectivity to N_2 at higher temperatures.

Overall, studies on copper modified clays have not provided suitable catalysts for operation temperature below 400 °C. Among the described materials, the most promising results could be achieved with copper containing hydrotalcite originated mixed metal oxides calcined at relatively low temperature. Though, the catalytic performance of these materials can be improved by their modification with small amounts of noble/rare earth metals.

5. Bi-functional catalysts

As stated above, it is still a great challenge to achieve both complete ammonia conversion at relatively low temperature and high selectivity to N_2 by using low cost catalysts. Therefore, recent developments mainly aimed at combining the advantages of two types of metals, i.e. noble/rare earth and transition metals deposited on one support (e.g. [75,123]) or in the form of mixed catalysts such as supported metal and metal-exchanged zeolites (e.g. [126,148]). For the latter group of catalysts also an application in form of a dual-layer or as mixed (washcoat) catalyst has been considered.

The concept of bi-functional catalysts is based on the internal selective catalytic reduction (*i-SCR*) mechanism of NH_3-SCO discussed in detail in Section 7. According to literature data, noble/rare earth metals present the components active in the oxidation of ammonia into NO (e.g. [79,150,151]), while transition metal oxides are mainly active for the selective reduction of NO with ammonia (NH_3-SCR) [87,144,152–154]. Consequently, a proper ratio of both metals is a crucial factor to adapt the relative reaction rates of both processes and optimize activity and selectivity of the catalytic systems in NH_3-SCO.

Only a limited number of studies focussing on such bi-functional catalyst concepts include copper as an active component. Examples comprehend $Pt/Cu/Al_2O_3$ (e.g. [30,37,38,70,119]), $Ag/Cu/Al_2O_3$ (e.g. [75,76,128]), $Au/Cu/Al_2O_3$ [76] and $Pt(Pd)/Cu(Ni)/SiO_2$ [155]. Among these materials, especially $Pt/Cu/Al_2O_3$ has been widely investigated under different reaction conditions. In all cited references this catalyst is composed of Pt and Cu with 1.0 and 20.0 wt.% loading, respectively. Kušar et al. [119] studied $Pt/Cu/Al_2O_3$ in NH_3-SCO under both fuel-lean and fuel-rich conditions of simulated biogas. The results under fuel-lean conditions revealed total ammonia oxidation at 250 °C, however with very high formation of NO_x over the catalyst. A higher N_2 selectivity could be observed over $Pt/Cu/Al_2O_3$ under fuel-rich conditions, though only 60% conversion was reached at 350 °C. Also Burch and Southward [37,38] examined $Pt/Cu/Al_2O_3$ in simulated biogas under cyclic fuel lean/rich operation. Interestingly, they reported a selectivity to N_2 of about 94% at 200 °C under lean conditions, which is significantly superior to data reported previously [156–158].

Others ratios of Pt:Cu in a $Pt/Cu/Al_2O_3$ system were not established nor discussed in literature, while proper mixing of those two metals could produce catalysts with better catalytic performance. In combination with Cu some other active components were investigated, i.e. Ag: 5.0–10.0 wt.% and 2.5–10.0 wt.% were studied by Gang et al. [75] and Yang et al. [128]. Among them (7.5 wt.%)Ag/(2.5 wt.%)Cu/Al_2O_3 facilitated complete ammonia conversion at 300 °C with 95% selectivity to N_2, but the productivity of this sample was only around 0.35×10^{-6} mol(N_2) $s^{-1}\,g^{-1}$. An increase in silver loading resulted in activation of the catalyst, but caused also an increasing NO_x formation. Similar conclusions were found for 3.0–4.6 wt.% gold doped on Cu/Al_2O_3 [76]. An increase of the gold loading to 5.0 wt.% enabled not only a total oxidation of ammonia at 327 °C but also 95% selectivity to N_2. This effect can be correlated with parallel decreasing Cu:Al molar ratio, which for this catalyst was the lowest among 1:5(10,15) and reached 1:5 for the catalyst with best performance. Therefore, in case of this catalyst, CuO species could be more readily available and, consequently increase the importance of NO reduction with ammonia to nitrogen. Nevertheless, further detailed studies over such materials are required.

Besides these examples of bimetallic catalysts, a few attempts aimed for dual-layer catalysts (e.g. [53,159–161]) or mixed (washcoat) catalysts (e.g. [33,34,126,148,162]) (Fig. 6). In dual-layer catalysts, the lower catalyst layer contains noble metal based materials to oxidize ammonia, while the upper layer consists of an NH_3-SCR catalyst. The use of such an upper layer is motivated by the need to improve the selectivity to N_2 of noble metal containing catalysts (e.g. [79,159]). NO_x formed by unselective ammonia oxidation in the SCO layer diffuses back through the SCR layer above, where it can be selectively converted by residual ammonia into nitrogen. Overall, only few studies discussed such dual-layer approaches in the open literature [79,159,160]. Interestingly, no copper based systems were proposed yet. Instead examples of proposed catalytic systems include: Pt/Al_2O_3 and Fe-zeolite proposed by Scheuer et al. [53] and Colombo et al. [163] or Pt/Al_2O_3 and Fe/ZSM-5 investigated by Shrestha et al. [161]. Despite high catalytic activity of both catalysts with full ammonia conversion at about 250 °C, N_2O formed in significant quantities in the temperature range of 200–350 °C. Poor selectivity to N_2 was also reported over mixed washcoat catalysts, such as Pt/Al_2O_3 and Cu/ZSM-5 [33] as well as Pt/Al_2O_3 and Cu/CHA [126,148,162]. Shrestha et al. [33] provided interesting insights into the basic working concept of dual-layer catalysts. They underlined the trend of increasing selectivity to N_2 with increasing copper loading of Cu/ZSM-5, in the same high temperature regime. Nitrogen oxide, which was generated in the underlying Pt/Al_2O_3 layer diffused into the Cu/ZSM-5 layer, where it reacted with counter-diffusing/stored NH_3 on catalytic sites active for NH_3-SCR to form N_2 [33]. For example, the selectivity to N_2 increased from 58 to 82% for 0.8 and 2.5 wt.% of Cu, respectively. Apparently, an optimum copper loading enables a high ammonia conversion and N_2 selectivity over the studied temperature range of 250–500 °C. Further studies in this direction appear promising.

Interestingly, Colombo et al. [163] compared a dual-layer of Pt/Al_2O_3 and Fe-zeolite with its mechanical mixture in order to find the role of such combinations on the catalytic performance in ammonia oxidation. Below 250 °C, catalytic activity was higher over the mechanically mixed catalytic system, while both catalysts revealed total ammonia conversion at temperatures above 250 °C. Interestingly, the selectivity to N_2 was higher over the mechanical mixture. This effect was explained by intimate contact between

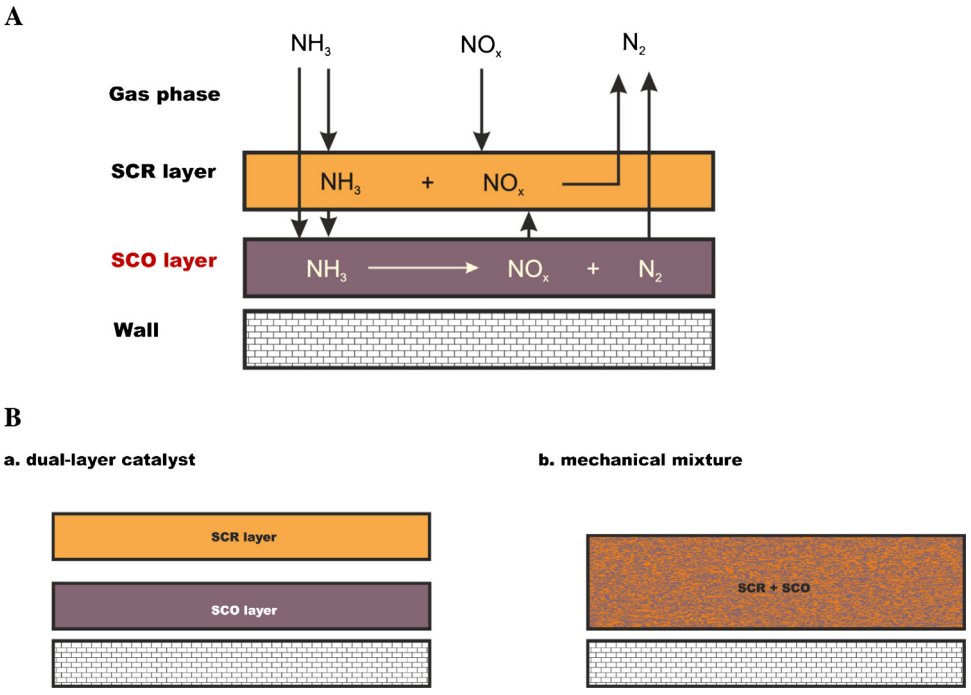

Fig. 6. Scheme of the dual layer catalyst concept (A). Adapted from Ref. [53], copyright granted by Elsevier; schematic comparison of dual-layer and mechanically mixed catalyst systems (B). Adapted from Ref. [163], copyright granted by Elsevier.

active species dedicated for both NH_3-SCO and NH_3-SCR processes, and consequently shorter diffusion length. Therefore, higher catalytic performance was obtained in comparison to a dual-layer catalyst were two catalysts were segregated. The authors compared these experimental data with predictive model simulations. They applied a heterogeneous one-dimensional dynamic plug-flow reactor model, which assumes the catalysts bed to be isothermal and isobaric. The simulation of the dual-layer monolith catalyst relied on a 1D + 1D reactor model accounting at each axial location for: (i) diffusion—reaction of SCR reactants and products inside the SCR catalyst layer (using SCR kinetics) and (ii) reaction at the SCO catalyst surface (using SCO kinetics), therefore in this case the two catalysts were actually segregated. Contrarily, simulation of the physical mixture of the two catalysts was done with a reactor model assuming superposition of the two catalytic kinetics operating in parallel. The presented simulation results satisfactory corresponded with that obtained during experimental studies. Therefore, the applied model can be used successfully for designing such catalytic systems.

Additionally, it should be stressed that a different behaviour of Fe- or Cu-exchanged zeolites appeared in NH_3-SCR. Nedyalkova et al. [164] observed an overconsumption of NH_3 in NH_3-SCR between 250 and 400 °C over Fe-Beta. Such an effect has already been reported earlier and is called *unusual parasitic ammonia oxidation* in the work of Kamasamudram et al. [165]. This effect comprehends following: (i) no nitric oxide was detected in direct ammonia oxidation with O_2 over tested Fe-zeolite, (ii) on the other side, ammonia was oxidized to nitrogen oxide; however, only in the presence of NO. The authors suggested a reaction of ammonia with an oxygen-containing intermediate formed during SCR. The intermediate was suggested oxidizing further with oxygen, while the produced NO was suggested reacting further with unreacted ammonia accompanied by formation of nitrogen [164]. As opposite to the iron-zeolite catalyst, the overconsumption of ammonia (up to 20%) during NH_3-SCR did not appear over copper-exchanged zeolites. Stoichiometric consumption appeared for several copper zeolites, such as Cu-Beta (e.g. [165–167]) and Cu-ZSM-5 (e.g. [168]). Therefore, another explanation is related to the possibility that NO could modify the oxidation state of the exchanged iron sites in the zeolite leading to their increased activity in ammonia oxidation. In contrast, an influence of NO on the copper oxidation state is very unlikely. Consequently overconsumption during NH_3-SCR did not appear. However, as stayed above such studies were conducted only over a limited number of zeolites; therefore, a mechanistic understanding and analysis of the nature of active species under the employed reaction conditions are certainly required. This issue definitely needs to be further evaluated.

In summary, only selected examples of bimetallic, dual-layer or mixed (washcoat) catalysts for NH_3-SCO are available in literature. Considering the reported activity and selectivity, such concepts appear highly attractive. Therefore, further research in this direction seems necessary, e.g. to elucidate potential synergistic effects of bimetallic catalysts, the influence of the support material and its structure as well as the nature of the catalytically active species under operation conditions.

6. Effects influencing catalyst performance

There are several factors that strongly influence the final performance of catalysts in NH_3-SCO such as: (i) the catalyst composition including metal loading (e.g. [90,103,120]), (ii) catalyst preparation e.g. the choice of metal and its precursor (e.g. [89]), preparation technique (e.g. [99]) as well as calcination temperature and time (e.g. [147]), (iii) redox properties of particular metal oxide species (e.g. [107,147]), (iv) surface acidity (e.g. [76,125]), (v) feed composition differing in NH_3:O_2 ratio (e.g. [70,127]) and presence of other exhaust gas components such as H_2O, SO_x, CO_x (e.g. [70,89,155]), etc. The effect of these parameters will be discussed for copper containing catalysts. Special attention will be devoted to copper amount and redox properties of catalysts, available acid sites as well as the influence of O_2, H_2O and SO_2 on the catalytic performance. Only a limited number of studies investigated the catalytic

Table 4
Review of catalytic performances of copper based catalysts for selective ammonia oxidation into nitrogen and water vapour (NH_3-SCO) in the presence of water vapour and sulphur oxide.

Pos.	Catalyst code	T (°C)	NH_3 conversion (%)	N_2 selectivity (%)	Productivity** (10^{-6} mol s^{-1} g^{-1})	Ref.
1	Cu/Al_2O_3 (450 °C, air-calc.) (3.4 wt.% Cu)	325	69	89	9.87	[107,118]
	(with 1.0% H_2O)		27	94	4.08	
2	Cu/Al_2O_3 (600 °C, air-calc.) (10.0 wt.% Cu)	350	100	90	2.85	[90]
	(with 5.2% H_2O)		100	95	3.01	
3	Cu/Al_2O_3 (800 °C, air-calc.) (20.0 wt.% Cu)	400	81	–	*	[119]
	(with 3.9 wt.% H_2O)		65	–	*	
4	Cu/TiO_2 (450 °C, air-calc.) (10.0 wt.% Cu)	250	100	95	0.71	[120]
	(with 3.0 wt.% H_2O)	350	100	97	0.72	
5	$CuO–CeO_2$ (500 °C, air-calc.) (6.0 mol% Cu)	350	–	–	*	[101,139]
	(with 12.0% H_2O)		87	80	0.79	
	(with 18.0% H_2O)		79	–	*	
6	CuO/La_2O_3 (500 °C, air-calc.) (8.0 mol% Cu)	350	–	–	*	[98]
	(with 12.0% H_2O)		72	53	0.43	
7	Cu/Y (400 °C, air-calc.) (8.4 wt.% Cu, NaOH treatment)	300	100	98	3.1	[90]
	(with 5.2% H_2O)		82	97	2.52	
8	Cu/Beta (450 °C, air-calc.) (3.0 wt.% Cu)	325	100	96	15.43	[107,118]
	(with 1.0% H_2O)		54	96	8.33	
9	$MgCuFeO_x$ (600 °C, air-calc.) (0.5 mol% Cu)	400	100	88	1.31	[122]
	(with 3.4% H_2O)		95	81	1.15	
10	$Pt/Cu/SiO_2$ (500 °C, air-calc.) (670.0 ppm Pt/10.0 wt.% Cu)	290	92	26	*	[155]
	(with 200 ppm SO_2)	293	92	97	*	
11	$Pt/Cu/Ni/SiO_2$(500 °C, air-calc.) (670.0 ppm Pt/10.0 wt.% Cu, Ni)	290	95	45	*	
	(with 200 ppm SO_2)	306	96	99	*	
12	$Pt/Pd/Cu/SiO_2$(500 °C, air-calc.) (670.0 ppm Pt, Pd/10.0 wt.% Cu)	290	95	39	*	
	(with 200 ppm SO_2)	328	100	99	*	
13	$Pt/Cu/Al_2O_3$ (450 °C, air-calc.) (1.0 wt.% Pt/20.0 wt.% Cu)	235	100	79	1.25	[70]
	(pretreatment with 100 ppm SO_2)		100	98	1.55	
	(with 8.0% H_2O)		100	89	1.4	
	(pretreatment with 100 ppm SO_2, 8% H_2O)		97	98	1.5	
14	$Pt/Cu/Al_2O_3$ (450 °C, air-calc.) (4.0 wt.% Pt/20.0 wt.% Cu)	235	100	84	1.33	
	(pretreatment with 100 ppm SO_2)		100	98	1.55	
	(with 8.0% H_2O)		100	95	1.5	
	(pretreatment with 100 ppm SO_2, 8% H_2O)		100	97	1.53	
15	Cu/ZSM-5 (500 °C, air-calc.) (4.4 wt.% Cu)	450	97	100	3.61	[105]
	(with 500 ppm SO_2, 4% H_2O)		65	–	*	

– not shown.
* not calculated.
** Calculated based on provided flow rates, NH_3 conversion and N_2 selectivity not considering volume change.

activity of materials in the presence of water vapour and sulphur oxide (Table 4).

6.1. Effect of copper loading

As mentioned above, the content of copper is an important factor, which significantly influences the performance of catalysts in selective ammonia oxidation into nitrogen and water vapour. Especially Gang et al. [90,103], He et al. [120], and Chmielarz et al. [122,144] focussed on this factor. For Cu/Al_2O_3, ammonia conversion increased significantly with increasing the copper loading from 5.0 to 10.0 wt.%. For higher loadings of up to 15.0 wt.%, no further increase of activity could be observed [90,103]. For Cu/TiO_2 the conversion remained stable for copper loadings from 10.0 to 20.0 wt.% [120], while a decreasing conversion was reported for $CuMgAlO_x$ hydrotalcite originated mixed metal oxides with copper loadings in the range of 5.0–20.0 mol% [144]. Therefore, based on these results it could be concluded that a copper amount around 10.0 wt.% was found to be the optimal loading, a number further proven by studies of Wang et al. [97] and Song et al. [142]. On the other hand, catalysts with lower copper concentration such as (1.3 wt.%)Cu/Al_2O_3 after H_2-pretreatment [29] and (3.7 wt.%)Cu/Y after NaOH treatment [90,103] were reported to exhibit outstanding catalytic performance and productivity among other catalysts, with was attributed to the high dispersion of CuO species in these materials.

Besides catalytic activity, the copper content also strongly affects the distribution of ammonia oxidation products, i.e. N_2, NO or NO_2 and N_2O. In general, a higher copper content results in a lower selectivity to N_2. Indeed, a certain optimum can be reached for small to medium copper loading and highly dispersed CuO species. At metal loading higher than 10.0 wt.%, copper dispersion could become poorer. Gang et al. [103] could neither by high-resolution transition electron microscopy (HREM) nor by ultraviolent spectroscopy (UV–vis–DRS) detect copper or CuO particles on alumina at loadings of 10.0 wt.% or lower emphasising highly dispersed copper oxide species. However, small particles of CuO with a size of around 5 nm were detected at 15.0 wt.% (Fig. 7). Though, in another study following a comparable synthesis procedure to obtain (10.0 wt.%)Cu/Al_2O_3, a CuO phase could be identified by XRD [131]. Also in case of (10.0 wt.%)Cu/TiO_2, a weak reflex attributable to crystallized CuO was observed [120]. Additionally,

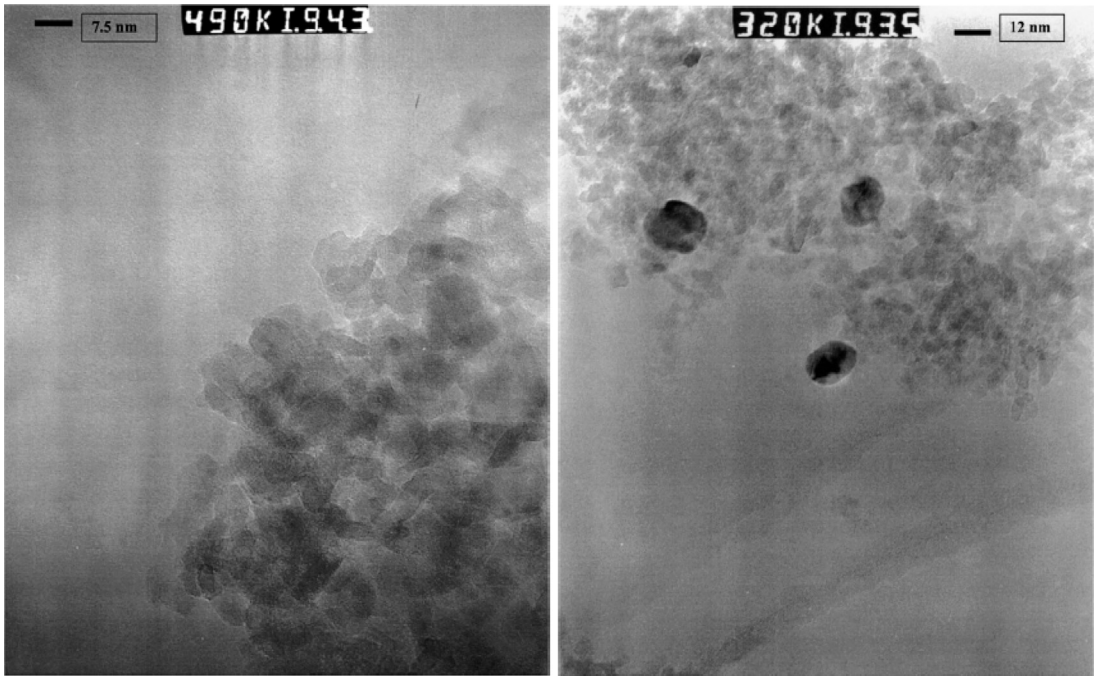

Fig. 7. High-resolution electron microscopy (HREM) images of the Cu/Al_2O_3 with 10.0 wt.% (left) and 15.0 wt.% of Cu (right). Reprinted from Ref. [103] with permission of Elsevier.

other reports emphasised CuO reflexes to become visible for more than 5.0 wt.% of copper (e.g. [169,170]).

6.2. Effect of redox behaviour

The redox properties of copper oxide present another factor influencing activity and selectivity in NH_3-SCO. Golodets et al. [171,172] and Slavinskaya et al. [173] suggested that the strength of the metal–oxygen bond in metal oxides determines the distribution of ammonia oxidation products. Oxides with high metal–oxygen bond strength exhibited lower rates of reaction and facilitated a high selectivity to N_2. In contrast, metal oxides with weak metal–oxygen bond strength led to the formation of NO_x (NO and N_2O). Chmielarz et al. [119] studied $Cu(Co,Ni,Fe)MgAlO_x$ hydrotalcite originated mixed metal oxides determining the strength of the metal–oxygen bond in transition metal oxides by temperature-programmed reduction (H_2-TPR). They observed a correlation between the reducibility of the transition metal oxides and the distribution of ammonia oxidation products, i.e. lower reducibility caused a lower selectivity to N_2. The only exception were mixed metal oxides containing copper, which could be reduced at significantly lower temperatures than the metal oxides mentioned above. The authors assign this deviation to parallel NH_3-SCR reactions of NO_x and unreacted ammonia forming nitrogen. Experiments confirmed significant activity of copper based materials in NH_3-SCR (e.g. [119,122,174]). However, a further increase of the copper loading from 5.0 to 20.0 mol% caused the formation of bigger metal oxide particles and decreased the oxygen bonding strength, leading to a decrease of the N_2 selectivity of $CuMgAlO_x$ [119]. The reducibility of supported copper oxides with different loading of copper was widely studied in the scientific literature (e.g. [175–177]). A general conclusion of these studies is that higher copper loadings (above 10.0 wt.%) result in a formation of bulk CuO species characterized by lower reducibility. More aggregated copper oxide species of lower reducibility were additionally found for (0.6 mol%)$CuMg(Zn)Al(Fe)O_x$ calcined at 900 °C. H_2-TPR analyses of these materials and of samples calcined at 600 °C together with the observed catalytic performance of the materials pointed towards higher catalytic activity in the low temperature range for materials with easily reduced CuO phases. Higher reducibility appeared to be accompanied by a high amount of exposed copper sites available for oxygen activation. An increase in calcination temperature resulted in a decrease of catalytic activity, possibly due to formation of more aggregated CuO species, which were less catalytically active in selective ammonia oxidation. On the other hand, the selectivity to N_2 depended on the various redox properties of copper oxide species present in those samples [147]. For example, higher selectivity to N_2 was found for $CuZnFeO_x$ catalysts calcined at 900 °C compared to materials prepared at 600 °C, which was connected with lower reducibility of CuO species present in the first sample. Therefore, it seems that the reducibility of copper oxide species is an important parameter in promoting an active and selective ammonia oxidation catalyst. Such a crucial role was not found for co-existing iron oxides species, which modified the catalytic performance of the catalysts only at high temperatures. In particular, Curtin et al. [107] found a linear relationship between the reduction temperature of CuO species and ammonia conversion for copper exchanged zeolite Beta, as depicted in Fig. 8. Obviously, the most active catalysts exhibited the lowest copper reduction temperature. Additionally, Wang et al. [97] found a correlation between the amount of finely dispersed CuO species and bulk CuO, and could show that a higher amount of finely dispersed copper oxide species resulted in a lower temperature for complete ammonia conversion over $CuO–CeO_2$.

A significant drop of the ammonia conversion occurred for a Cu/Beta catalyst after 1 h of wet ammonia oxidation with 1.0% of water vapour. The observation was ascribed to changes of the redox properties of the material [118]. Examples of H_2-TPR for fresh copper exchanged zeolites with a copper loading of 3.0 wt.% and after water exposure are summarized in Fig. 9. After water exposure, the high temperature peak increased significantly at the expense of the low temperature peak, showing that dispersed CuO species aggregated to form larger CuO species, which are characterized by lower reducibility. These species were less catalytically active for NH_3-SCO, but more selective to N_2. Therefore, for (3.0 wt.%)Cu/Beta ammonia conversion decreased in wet conditions not only due to

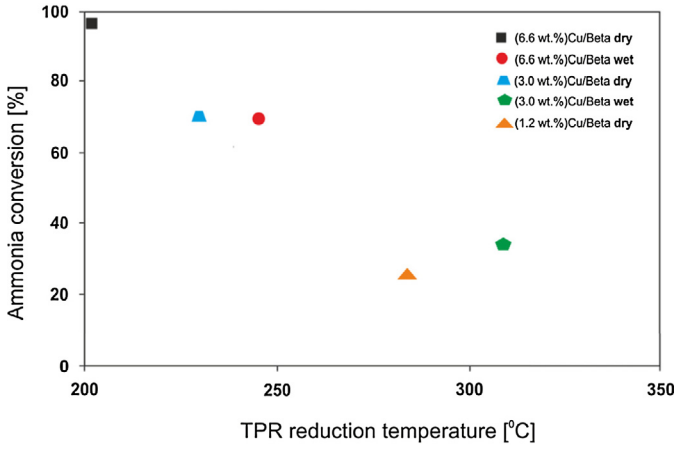

Fig. 8. Ammonia conversion with H_2-TPR reduction temperature of Cu/Beta. Reaction conditions: 0.54% NH_3, (1.0% H_2O), 8.0% O_2, balance He, 25 mg catalyst, W/F = 0.0075 g s ml^{-1}, 325 °C. Adapted from Ref. [107], copyright granted by Royal Society of Chemistry.

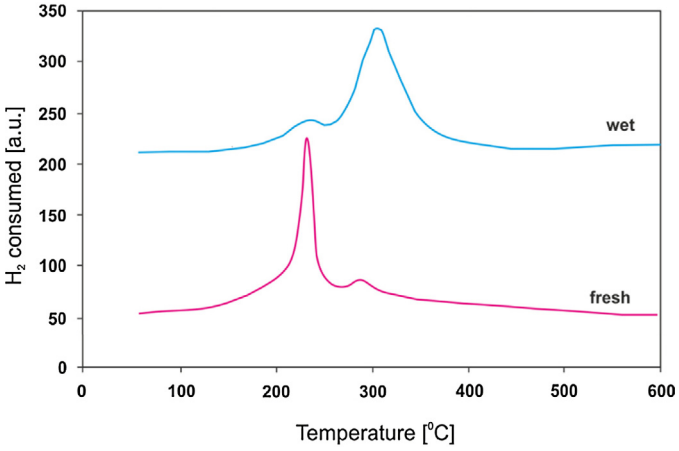

Fig. 9. H_2-TPR profiles of fresh (3.0 wt.%)Cu/Beta and (3.0 wt.%)Cu/Beta after 1 h of wet testing. Reaction conditions: 5.0% H_2, balance N_2, 35 mg catalyst, flow rate = 20 ml min^{-1}, ramp rate = 10 K min^{-1}. Adapted from Ref. [118], copyright granted by Elsevier.

competitive adsorption of ammonia and water on active sites but also due to a rearrangement of CuO species promoted in the presence of water vapour. Such material changes led to an irreversible loss of the activity of these materials. Further advanced investigation covering the CuO particle size and the oxidation state of copper oxide species before and after catalysis are required.

6.3. Effect of acid sites

Another factor that affects the activity in selective ammonia oxidation into nitrogen and water vapour is surface acidity. Il'chenko and Golodets [66,171,178] have compared the catalytic performance of a large number of catalysts and they concluded that acidic metal oxides, such as V_2O_5, MoO_3, WO_3, exhibited excellent selectivity to N_2 at low temperatures. Interestingly, these oxides present the key components of the industrial NH_3-SCR catalyst (e.g. [40,44]). In further studies, many researchers utilized Al_2O_3 (e.g. [78,118,127,129]) or aluminium modified materials (e.g. [122–124]), zeolites (e.g. [28,109,111,118]) or $H_3PW_{12}O_4$ (12-tungstophosphoric acid) [179], because of their acidity, which is advantageous in capturing ammonia close to the active species dispersed on the support surface. Ion exchanged zeolites were reported to exhibit comparable or slightly better catalytic activity compared to alumina supported oxides with the same metal loading (e.g. [28,90]). Yue et al. [121] reported higher selectivity to N_2 for mesoporous catalysts with higher specific surface area, i.e. a larger number of accessible acid sites, than on conventional materials. Additionally, they claimed that the existence of mesopores facilitated the transport of the reactant gas to access the active surface sites and thus enhanced ammonia adsorption and oxidation. Other catalysts with a higher amount of surface acid sites were reported to favour the catalytic oxidation of ammonia. For example, a significant increase of additional centres for ammonia chemisorption was reported after deposition of transition metal oxides (e.g. [125,180]). On such oxide species, ammonia can adsorb on both Brönsted and Lewis acid sites. Chmielarz et al. [125] reported that introducing copper oxide into PCHs (porous clay heterostructures) significantly increased the concentration of Lewis acid sites and decreased the quantity of Brönsted acid sites. The formation of Lewis acid sites was associated with an overall increase of the surface acidity of the Cu-PCH materials. In line, Darvell et al. [36] by applying FT-IR studies of pyridine and ammonia over a Cu/Al_2O_3 catalyst concluded that Lewis acid sites dominate and additionally ammonia adsorption on these sites appears likely to be the first step in NH_3-SCO. Neither on the surface of the Cu/Al_2O_3 nor on pure alumina any appreciable Brönsted acidity was detected [76]. These findings are consistent with previous works of Ramis et al. [96] and Amores et al. [181], who confirmed that Brönsted acidity was not required for NH_3-SCO. Lin et al. [76] gave an order of decreasing concentration of Lewis sites of metals supported on alumina as following: Cu > Al_2O_3 > Fe > Ti > Ce > Li. However, they found that this order did not counterpart the tendency of increasing activity in ammonia oxidation. Therefore, they suggested that differences in catalytic activity could not only be assigned to the Lewis acid site density on oxide surfaces. Consequently, the role of ammonia bonded to Brönsted acid sites, i.e. NH_4^+ ions as additional reservoir of ammonia chemisorbed cannot be excluded [182–185]. High N_2 selectivity, especially in the high temperature range, could indeed be related to protection of NH_4^+ ions against oxidation and therefore their availability for reduction of NO_x (NH_3-SCR) [106]. Nevertheless, further studies are necessary to identify the role of Brönsted and Lewis acidic sites of copper based catalysts in NH_3-SCO.

6.4. Effect of oxygen content

A majority of investigations on ammonia oxidation discussed in the open literature focusses on a NH_3 concentration in the range of 300–5000 ppm (e.g. [28,79,85,116,186,187]). Common NH_3:O_2 ratios used in these studies are 1:5 (e.g. [106,123,124]), 1:10 (e.g. [100,128,131]) or 1:20 (e.g. [37,54,105,142]). Investigations considering the influence of changes of the ammonia to oxygen molar ratio on the catalytic performance were only discussed in a limited number of publications (e.g. [29,70,127]). In general, a decreasing NH_3:O_2 ratio increased the activity but in parallel decreased the selectivity to N_2. In particular, Lippits et al. [29] studied three different NH_3:O_2 ratios including 1:1(5 or 25) over (1.3 wt.%)Cu/Al_2O_3 (Fig. 10). For this system, ammonia conversion started at 300 °C, while a total ammonia conversion was achieved at 400 °C with a NH_3:O_2 ratio of 1:1. A lower NH_3:O_2 ratio of 1:5, did not cause changes of the temperature onset, but total ammonia conversion was already reached at 350 °C. The highest catalytic activity resulted for a ratio of NH_3:O_2 = 1:25 with complete ammonia oxidation at 300 °C. Above 350 °C the oxygen content had no influence on N_2 selectivity. Below 350 °C, an opposite effect was observed and N_2 selectivity decreased for increasing oxygen content. On the other site, Olofsson et al. [70] presented higher activity and selectivity to N_2 with 0.5 compared to 8.0% O_2 (NH_3:O_2 = 1:7, 1:114), respectively, indicating competitive adsorption of ammonia and excess oxygen. Detailed studies to explore this effect are certainly

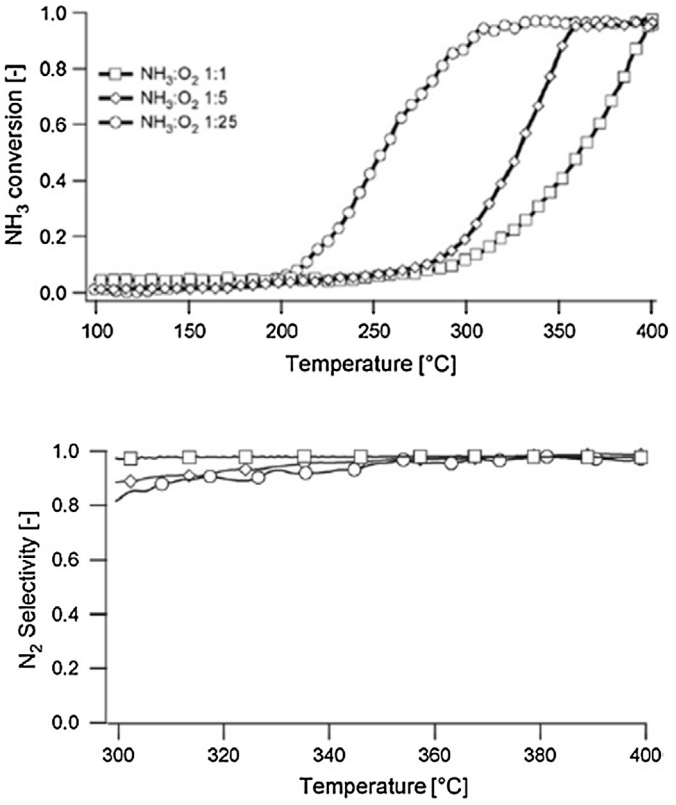

Fig. 10. Ammonia conversion and selectivity to N_2 over Cu/Al_2O_3 for different NH_3:O_2 ratios. Reaction conditions: 4.0% NH_3, 4.0–100.0% O_2, balance Ar, 200 mg catalyst, flow rate = 40 ml min^{-1}, GHSV = 2500 h^{-1}. Reprinted from Ref. [29] with permission of Elsevier.

required, mainly due to the high oxygen content of around 10% in exhaust gases emitted by diesel engines [188] together with a minor ammonia slip.

6.5. Effect of water vapour and sulphur oxide

Besides ammonia and oxygen, exhaust gases also contain other compounds such as water vapour, sulphur and carbon oxides. Thus, ammonia slip catalysts should exhibit sufficient activity in the presence of these compounds. Unfortunately, only a limited number of studies report a selective ammonia oxidation in the presence of these additional compounds. Table 4 summarizes these studies. In most cases, water vapour in the feed composition improved the selectivity to N_2 (e.g. [70,107,118,120]) but caused a decrease of the catalytic activity (e.g. [90,107,118]). Reduced activity induced by the presence of water vapour was associated with competitive adsorption of water and ammonia or by condensation of water vapour on the catalysts resulting in partial blocking of the active sites (e.g. [28,90,130]). Another potential explanation refers to aggregation of easily reducible CuO species as discussed in Section 6.2 [118]. Lenihan and Curtin [118] conducted temperature programmed desorption experiments (NH_3-TPD) revealing two ammonia desorption regions at 80–150 and 210–300 °C over (3.4 wt.%)Cu/Al_2O_3 (Fig. 11). After passing H_2O over catalysts with preadsorbed ammonia, the low temperature desorption peak in the NH_3-TPD profile disappeared. However, the high temperature desorption peak remained, and therefore, they claimed that weakly adsorbed ammonia was displayed by water vapour. Moreover, the study confirmed the importance of weakly adsorbed ammonia for NH_3-SCO and emphasized a competition adsorption of ammonia and water on the catalytically active sites. However, the

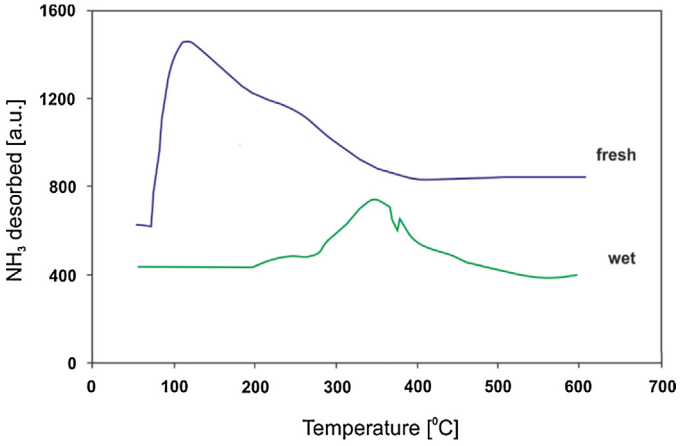

Fig. 11. Comparisons of NH_3-TPD with and without water treatment for Cu/Al_2O_3. Reaction conditions: 4.0% NH_3, (1.0% H_2O), balance He, 150 mg catalyst, flow rate = 20 ml min^{-1}, ramp rate = 10 K min^{-1}. Adapted from Ref. [118], copyright granted by Elsevier.

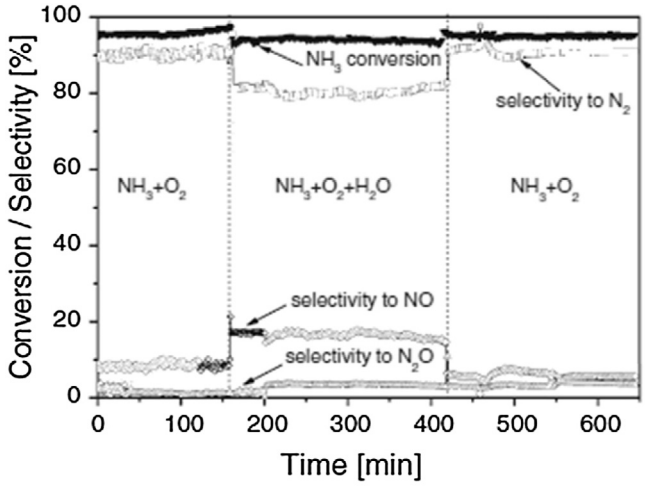

Fig. 12. Ammonia conversion and selectivity to N_2 over $MgCuFeO_x$. Reaction conditions: 0.5% NH_3, 2.5% O_2, (3.4%H_2O), balance He, 100 mg catalyst, flow rate = 40 ml min^{-1}, GHSV = 15,400 h^{-1}, 400 °C. Reprinted from Ref. [122] with permission of Springer.

(3.4 wt.%)Cu/Al_2O_3 catalyst was only reversibly altered in the presence of water vapour and the catalytic activity could be restored. N_2 selectivity slightly increased in the presence of H_2O accompanied by decreased NO_x formation. Especially N_2O formation was suppressed in the presence of water vapour [107,118]. Also Chmielarz et al. [122] confirmed a reversible deactivation of $MgCuFeO_x$ hydrotalcite originated mixed metal oxides caused by H_2O in the reaction mixture. After removal of water vapour from the feed gas, no significant change of the catalyst performance was observed (Fig. 12). Comparison of the obtained results with other presented in the scientific literature have shown significantly lower deactivation in the presence of water vapour of $MgCuFeO_x$ mixed metal oxides than Cu/TiO_2 (e.g. [120]) or Cu/Al_2O_3, Cu/Y (e.g. [90,103,118]). Unfortunately, no comprehensive characterization of the catalysts after application in the presence of water vapour, e.g. including specific surface area, XRD or H_2-TPR was presented hampering interpretation of the reported behaviour.

As stated above, copper exchanged zeolite Beta—(3.0 wt.%)Cu/Beta, exhibited superior catalytic activity for the selective ammonia oxidation but proved to be unstable in the presence of water vapour [107,118]. Interestingly, a higher copper loading reduced this negative influence, i.e. copper exchanged

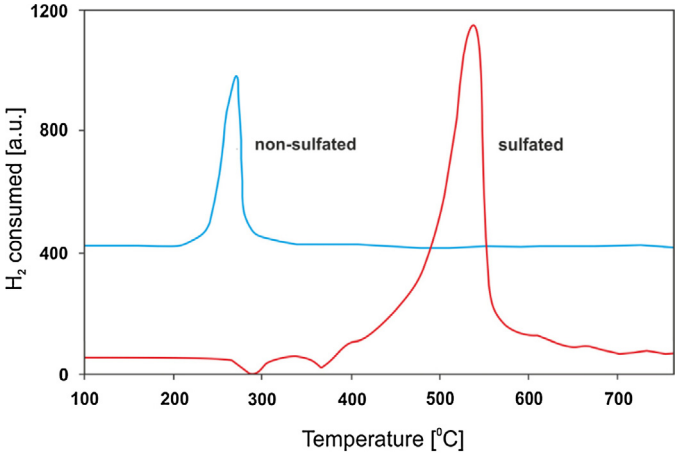

Fig. 13. H_2-TPR profiles of fresh (3.4 wt.%)Cu/Al_2O_3 and (3.4 wt.%)Cu/Al_2O_3 after exposure to SO_2. Reaction conditions: 5.0% H_2, balance N_2, 35 mg catalyst, flow rate = 20 ml min^{-1}, ramp rate = 10 K min^{-1}. Adapted from Ref. [87], copyright granted by Elsevier.

zeolite Beta with 6.6 wt.% of copper exhibited higher stability of the catalytic activity in the presence of H_2O [107]. Unfortunately, no H_2-TPR results were shown to provide information on the reducibility of the CuO species of the materials. The reducibility of materials after wet ammonia oxidation should undergo further investigation also in case of other copper based materials applied for NH_3-SCO.

Also a sulphur oxide treatment of catalysts or SO_2 in the feed influences the catalytic performance of potential NH_3-SCO catalysts. Catalytic tests of different types of materials emphasized a positive effect of sulphate species on N_2 selectivity (e.g. [70,87]). Cu/TiO_2 prepared based on different precursors, such as $CuSO_4$ and $Cu(NO_3)_2$, respectively, showed higher selectivity to N_2 for the former precursor [89]. A comparable effect occurred in case of Fe_2O_3 mixed oxides prepared form iron sulphate [84]. Curtin et al. [87] introduced SO_2 to the reaction stream and reported a beneficial effect on N_2 selectivity together with reduced activity. Jeong et al. [189] provided a comparison of ammonia oxidation over fresh and sulphated Cu(8.0 wt.%)/Al_2O_3. The sulphated catalysts required around 100 °C higher temperature for total ammonia conversion compared to the fresh sample. The authors suggested, that below 300 °C ammonia could not be oxidized over sulphated catalysts but it was adsorbed on the sulphate surface of the catalysts to produce $(NH_4)_2SO_4$. Above 327 °C $(NH_4)_2SO_4$ decomposed to produce SO_2 followed by oxidation of NH_3 to N_2 and small amounts of NO [189]. Jones et al. [127] reported an increasing ammonia conversion over (10.0 wt.%)Cu/Al_2O_3 in the presence of H_2S in the gas mixture at 700 °C, with excellent selectivity to N_2. Moreover, also for Cu/SiO_2 a significantly improved selectivity to N_2 could be observed when adding SO_2 to the feed. Dannevang [155] patented a process for the catalytic low temperature oxidation of ammonia in the off-gas at temperatures of 200–500 °C. They claimed that the catalytic performance of Pt(Pd)/Cu(Ni)/SiO_2 considerably improved by adding small amounts of sulphur oxide to the feed composition. The presence of SO_2 in the gas resulted in superior N_2 selectivity during ammonia oxidation. For example by applying $Pt/Pd/Cu/SiO_2$, the selectivity to N_2 rose from 39 to 99% by sulphation. Unfortunately, a comprehensive characterization of the investigated materials [127,155,189] was not provided to elucidate the origin of this behaviour. Curtin et al. [87] discussed a correlation of the catalytic performance of tested materials to their redox properties. H_2-TPR profiles of fresh (3.4 wt.%)Cu/Al_2O_3 and after exposure to sulphur oxide are presented in Fig. 13. A shift of the maximum peak from 250 to 520 °C for the sulphated catalyst confirmed a major change in reducibility. Higher selectivity to N_2 for sulphated samples was explained by formation of surface sulphates stabilizing the oxide anions in the CuO lattice, and thus generating higher oxygen bonding strength (e.g. [144,172,173]).

The effect of water vapour in combination with sulphur oxide in the reaction mixture was also studied. Olofsson et al. [70] reported that a SO_2-pretreatment led to a minor deactivation associated with considerably improved N_2 selectivity. Catalytic tests over (1.0 or 4.0 wt.%)Pt/(20.0 wt.%)Cu/Al_2O_3 revealed no effect of the SO_2-pretreatment on the conversion for dry conditions. The conversion remained at 100%, whereas the selectivity to N_2 increased from 79–84% before to 98% after the pretreatment. Under wet conditions a small decrease in conversion from 100 to 97% could be observed for a catalyst with 1.0 wt.% loading of platinum. However, for both catalysts the selectivity to N_2 increased by a few percent and reached about 97–98% after the SO_2-pretreatment. The decreasing activity of the catalyst tested under feed containing water vapour was explained similar to previous reports by competitive adsorption between ammonia and water. A replacement of some of the active oxygen sites by sulphate species was named causing the observed loss of catalytic activity. In turn, the selectivity to N_2 increased due to decreased oxidation ability of the catalyst, but also due to higher surface acidity, i.e. an increase of the concentration of Lewis acid sites. However, the studies did neither provide information on the concentration of Lewis acid sites nor H_2-TPR properties of fresh, sulphated and/or wet samples. Detailed studies covering the acid/base and redox properties of materials under different reaction conditions are certainly necessary to elucidate the origin of the discussed changes of catalytic activity and selectivity in the presence of water vapour and SO_2. A comprehensive understanding of structure-performance correlations under realistic reaction conditions for ammonia slip catalyst could pave the way for a knowledge driven catalyst optimization.

7. The mechanisms of NH_3-SCO

In order to facilitate a rational design of active and selective catalysts, the elementary surface reaction steps need to be identified. At the moment, three mechanisms have been investigated and reported in the scientific literature: (i) the imide mechanism [190], (ii) the hydrazine mechanism (e.g. [30,36,88,96,120,130,146,181]) and (iii) the internal selective catalytic reduction (*i-SCR*) mechanism (e.g. [32,37,38,89,96,105,109,111,138,144,179,191]). A detailed description of these mechanisms was given by Jabłońska et al. (e.g. [52,149]). The mechanism of selective ammonia oxidation into nitrogen and water vapour is still uncertain. However, a majority of researchers agree that NH_3-SCO proceeds via (iii) the *i-SCR* mechanism, which consists of two reaction steps. In the first step, ammonia is partially oxidized to nitrogen oxide, while in the second step, nitrogen oxide is reduced to N_2 and/or N_2O by ammonia unreacted in the first step, according to Eqs. (1), (3), and (4):

$$\text{Step1}: 4NH_3 + 5O_2 \rightarrow 4NO + 6H_2O \quad (3)$$

$$\text{Step2}: 4NO + 4NH_3 + O_2 \rightarrow 4N_2 + 6H_2O \quad (1)$$

$$4NO + 4NH_3 + 3O_2 \rightarrow 4N_2O + 6H_2O \quad (4)$$

Detailed studies of the reaction mechanism using temperature programed techniques (NH_3-TPD, NH_3-TPSR) (e.g. [103,122]), catalytic tests (NH_3-SCO with various space velocities, NH_3-SCO under lean/rich conditions, NH_3-SCR) (e.g. [37,122,123]) as well as transient response (e.g. [30]) and spectroscopic studies (FT-IR) (e.g. [106]) were carried out. Based on NH_3-TPD measurements over copper based catalysts, Chmielarz et al. [122] and Gang et al. [103] concluded that both surface and lattice oxygen reacted with NH_3 to produce N_2 and N_2O, but surface oxygen was found to be much

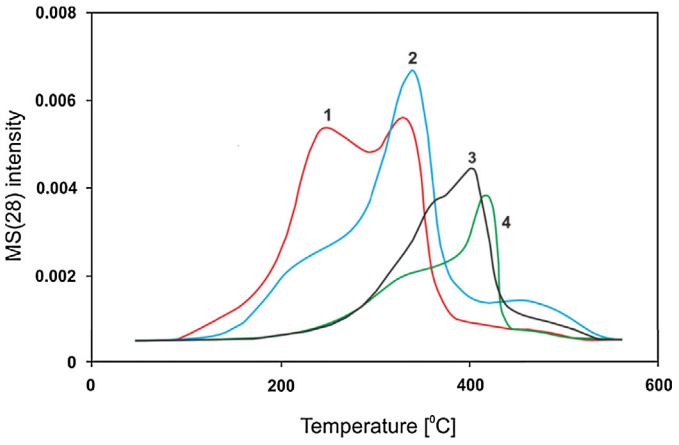

Fig. 14. N_2 production profiles on an oxidized Cu/Al_2O_3 during NH_3-TPD (obtained during four consecutive NH_3 exposures). Reaction conditions: 1.14% NH_3, (8.21% O_2, 500 °C, 2 h, before first cycle), balance He; 200 mg catalyst; flow rate = 74.7 ml min^{-1}, ramp rate = 5 K min^{-1}. Adapted from Ref. [103], copyright granted by Elsevier.

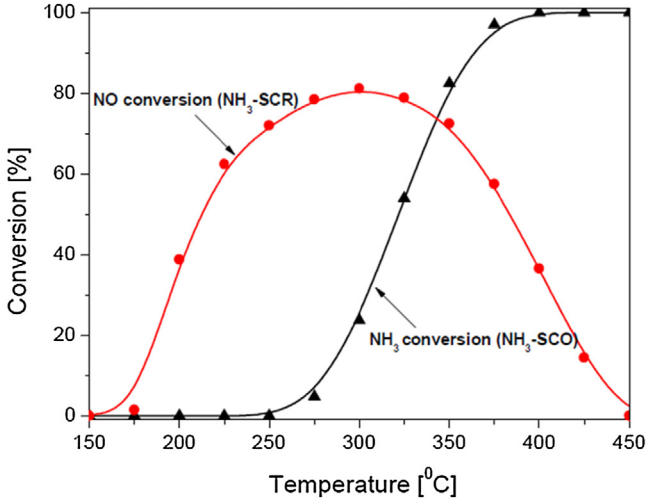

Fig. 15. Ammonia conversion and nitrogen oxide conversion over $MgCuFeO_x$. Reaction conditions: 0.5% NH_3 (in NH_3-SCR: 0.25% NH_3, 0.25% NO) 2.5% O_2, balance He; 100 mg catalyst; flow rate = 20 ml min^{-1}, GHSV = 15,400 h^{-1}. Adapted from Ref. [149], copyright granted by Chemik International.

more active than lattice oxygen at low temperatures. In particular, studies conducted over oxidized Cu/Al_2O_3 revealed the formation of N_2 over four sequential cycles [103], as shown in Fig. 14. For the first cycle, two peaks with a maximum at around 250 and 330 °C were detected, while for the next cycles this first peak disappeared while the second peak shifted sequentially to higher temperatures with every successive cycle. Formation of N_2 in the first maximum was attributed to a reaction between ammonia and adsorbed surface oxygen, which was almost totally consumed after the first NH_3-TPD cycle. The second maximum was caused by reaction of ammonia with lattice or possibly subsurface oxygen. A similar hypothesis was made for oxidized copper exchanged zeolite Y. However, in this case N_2 only formed in the first cycle, an observation which was explained by the absence of oxygen on Cu/Y or total reduction of copper oxide species after the first cycle of NH_3-TPD experiments [103].

Apart from the evolution of N_2 and N_2O, also NO was detected during NH_3-TPSR measurements over $MgCuFeAlO_x$ catalysts [122]. Nitrogen oxide was produced for these samples only in the high temperature range of 350–500 °C, in which there was no chemisorbed ammonia able to convert nitric oxide to N_2 and/or N_2O. These results were additionally supported by catalytic tests of ammonia oxidation with various space velocities. An increase in space velocities (SV) shifted the ammonia conversion curves to higher temperatures as well as increased selectivity to NO and consequently decreased selectivity to N_2, especially at higher temperatures [87,119,122,144]. For the tests performed with a relative low space velocity, the contact time of reactants with the catalysts surface was long enough for both reaction steps, i.e. ammonia oxidation to NO and NO reduction by unreacted ammonia. In contrast, for experiments performed with increased space velocity, the contact time was too short for effective reduction of NO by ammonia, and consequently, the selectivity to NO increased. Therefore, the obtained results confirm NO as primary product and a reduction to N_2 by NH_3-SCR.

Comparisons of NH_3-SCO and NH_3-SCR over the same catalyst [122,149] revealed a conversion of NO via NH_3-SCR at lower temperatures than a conversion of ammonia via NH_3-SCO (Fig. 15). In line, the oxidation of ammonia to NO (step 1, Eq. (3)) seemed to present the rate-determining step in the low temperature range [122,149], a finding which supports the hypothesis that the selective oxidation of ammonia into nitrogen and water vapour proceeds according to the *i-SCR* mechanism. The relative rate of both steps was found to be a crucial factor determining the selectivity of the whole process. A higher rate of ammonia oxidation to nitrogen oxide resulted in lower selectivity to N_2, while a higher rate of NO reduction by ammonia led to higher selectivity to N_2 but also lower catalytic activity [123,149].

Besides the catalytic systems mentioned above, the *i-SCR* mechanisms was proposed for a large number of catalysts including copper based systems, such as CuO/Al_2O_3 [87], $Ag/Cu/Al_2O_3$ [75], $Pt/Cu/Al_2O_3$ [37], $MgCu(Co)Fe(Al)O_x$ [122,123,144,147] or $(Pt,Pd,Rh)/MgCuFe(Al)O_x$ [123], etc. High catalytic performance of the mentioned catalysts in the selective catalytic reduction of NO with ammonia (NH_3-SCR, $DeNO_x$) provided an additional evidence for the *i-SCR* mechanism in NH_3-SCO (e.g. [97,122,123,144,147]). Additionally, a large number of studies demonstrated copper based catalysts as the most active and selective for NH_3-SCR (step 2) (e.g. [87,144,152–154,192–198], etc.). On the other side, noble metals are known to be active catalysts of ammonia oxidation to NO and water vapour, and well known from the so called Ostwald process (step 1), which is one of the stages in nitric acid production (e.g. [199–201]). Numerous papers were published (e.g. [93,173,202,203]) suggesting the subsequent dehydrogenation of ammonia: $-NH_3 \rightarrow -NH_2 \rightarrow -NH \rightarrow -N$, until the formation of N_{ads} species, which interact with O_{ads} to produce NO (e.g. [204–207]) and NO_2 [30], while the formation of N_2 occurs by interaction of two N_{ads} species [138] over noble metals. Recently, Cui et al. [138] proposed a synergistic catalytic effect between RuO_2 and CuO during ammonia oxidation suggesting that coordinatively unsaturated Ru atoms (cus), present in RuO_2 can easily adsorb and activated NH_3 molecules and oxygen atoms. Similar concepts have been proposed for CeO_2 in $CuO–CeO_2$ mixed oxides systems [97]. Such adsorbed species can be converted in a sequence of reactions illustrated in Eq. (5):

$$NH_{3\text{-cus}} + O_{\text{-cus}} \rightarrow (NH_2)_{ad} + OH_{ad} \rightarrow N_{\text{-cus}} + H_2O \quad (5)$$

In the next step, the $N_{\text{-cus}}$ species may recombine with each other to form N_2 or with $O_{\text{-cus}}$ into $NO_{\text{-cus}}$ according to Eqs. (6) and (7), respectively:

$$N_{\text{-cus}} + N_{\text{-cus}} \rightarrow N_2 \quad (6)$$

$$N_{\text{-cus}} + O_{\text{-cus}} \rightarrow NO_{\text{-cus}} \quad (7)$$

Therefore, the activity and selectivity to N_2 of the process depended on the density and distribution of $N_{\text{-cus}}$ and $O_{\text{-cus}}$ species on the catalyst surface. However, the presented mechanism did not

explain N_2O and NO_2 formation. In former investigations of Burch and Southward [38], no differentiation was made between NO and NO_2, while a study of Gang et al. [75] assumed the reacting NO_x species as NO. On the other hand, Olofsson et al. [30] used a transient response study revealing that the reacting NO_x species was NO_2 instead of NO. This finding is in agreement with reports of Curtin et al. [87], in which they showed NO_2 besides NO as a product of the overoxidation of ammonia over Cu/Al_2O_3. Obviously, a careful analysis of the product spectrum is necessary, especially with regard to the first step (Eq. (3)) of ammonia oxidation.

Furthermore, Cui et al. [138] suggested that CuO could selectively reduce NO_{-cus} species adsorbed on the RuO_2 surface to N_2 according to Eq. (8):

$$NO_{-cus} + NH_{3-cus} \rightarrow N_2 + H_2O \quad (8)$$

Indeed, copper oxide species were reported to be less active in ammonia oxidation than noble metals (e.g. [123,128]). Thus, dehydrogenation of chemisorbed NH_3 molecules should be slow. Therefore, a significant population of NH_{3-x} species on their surface could be expected [30]. Such species were reported to react with NO to form N_2 and/or N_2O [205,206,208,209]. Experiments of Burch and Southward [37] emphasized that under rich conditions (NH_3:O_2 = 1:1), CuO was partially reduced by ammonia to produce a reservoir of NH_{3-x} species. Then, on switching to lean conditions (NH_3:O_2 = 1:21), ammonia from the gas phase was again fully oxidized to NO on the active sites of Pt/PtO_x and subsequently reduced to N_2 by NH_{3-x} on copper oxide species. However, this reduction process was found to be limited by the concentration of NH_{3-x} species, i.e. when they were consumed, an excess of NO was observed. A potential explanation refers to oxygen consumption during NH_3-SCO. Ammonia oxidation to N_2 proceeds with a ratio of NH_3/O_2 = 1.33 (Eq. (2)). Another possible product of ammonia oxidation is N_2O which is form according to Eq. (9):

$$2NH_3 + 2O_2 \rightarrow N_2O + 3H_2O \quad (9)$$

For the formation of N_2O, equal amounts of ammonia and oxygen are consumed (NH_3/O_2 = 1.00). In contrast, the oxidation of ammonia to NO (Eq. (3)) requires a higher oxygen concentration (NH_3/O_2 = 0.80).

The *i-SCR* mechanism was also proposed for a Cu–Ru system [138] and other bimetallic catalysts (e.g. [37,38,75,123]), however, it seems that it can be valid also in case of other combinations of noble/rare earth and transition metals. Associated with this mechanism is a clear need for the design of catalysts merging appropriate catalytically active sites for both reaction steps 1 and 2, respectively. However, note that the *i-SCR* mechanism has been proposed without taking into account the effect of the presence of other exhaust gases, such as H_2O, SO_x, CO_x. Consequently, the *i-SCR* mechanism could be modified under more realistic feed gas compositions. Therefore, advanced studies of the reaction mechanism under real conditions are highly desirable.

8. Conclusions

Nitrogen oxides (NO, NO_2) are mainly produced during the combustion of fuel from stationary and mobile sources. The selective catalytic reduction of NO_x with ammonia (NH_3-SCR, $DeNO_x$) is the most important as well as well-established process used to abate NO_x. A high efficiency of NO_x removal requires a stoichiometric or even access of urea injection and adding a layer of ammonia slip catalyst able to selectively oxidize ammonia into nitrogen, without introducing other reactants into the gas mixture. On the other hand, the design of active, selective and stable catalysts presents a great challenge. Clearly, the most efficient catalysts for selective ammonia oxidation into nitrogen and water vapour (NH_3-SCO) are copper based systems. In particular, a high catalytic performance was found over alumina supported copper catalysts and copper exchanged zeolites. Further investigations of these materials seem to be reasonable in order to find promising candidates of ammonia slip catalysts for industrial application. Catalytic systems with a high dispersion of copper oxide species enable ammonia oxidation at low temperatures with high selectivity to N_2 and productivity. An optimization of preparation methods facilitating a high dispersion of copper oxide appears promising. An interesting concept is an alkaline treatment, e.g. with NaOH. Besides redox properties of catalysts also acidity plays an important role in selective ammonia oxidation due to the possible activation of ammonia molecules in adsorbed form. Unfortunately, the role of Lewis and Brönsted acidity is still not clear, and more research in this direction should proceed.

The activity of copper based catalysts can be improved by addition of small amounts of noble metals, unfortunately associated by a decrease in selectivity to N_2. A suitable proportion of copper and noble/rare earth metals such as platinum, palladium or cerium should allow producing highly efficient bi-functional, i.e. bimetallic, dual-layer or mixed (washcoat) catalysts. Note, that both dual-layer or mixed (washcoat) catalysts are relatively new concepts.

In addition to the requirements of high activity, selectivity to N_2 and stability, the effects of oxygen ratio, presence of water vapour and sulphur oxide continue to pose practical challenges for NH_3-SCO and should be investigated further. It is clear that additional research under real conditions is needed to select catalytic systems applicable for commercial use. As summarized in this review, although significant progress has been made in the design of ammonia slip catalysts, there are some gaps concerning catalyst characterization necessary for a fundamental understanding of the observed catalyst behaviour. The same conclusion is also valid concerning the proposed *i-SCR* mechanism. The main evidence for this mechanism was obtained under conditions that are far from the real conditions of low temperature ammonia oxidation. In line, a targeted materials design will rely on a comprehensive understanding of the elementary reactions occurring under real reaction condition.

Acknowledgement

Funded by the Excellence Initiative of the German federal and state governments in the frame of the *Center for Automotive Catalytic Systems Aachen* (ACA) at RWTH Aachen University.

References

[1] K. Na, C. Song, C. Switzer, D.R. Cocker, Environ. Sci. Technol. 41 (2007) 6096–6102.
[2] G. Busca, C. Pistarino, J. Loss Prevent. Proc. Ind. 16 (2003) 157–163.
[3] H.H. Ou, C.H. Liao, Y.H. Liou, J.H. Hong, S.L. Lo, Environ. Sci. Technol. 42 (2008) 4507–4512.
[4] Q. Geng, Q. Guo, C. Cao, Y. Zhang, L. Wang, Ind. Eng. Chem. Res. 47 (2008) 4363–4368.
[5] K.E. Noll, V. Gounaris, W.S. Hou, Adsorption Technology for Air and Water Pollution Control, sixth ed., Lewis, Chelsea, 1991.
[6] S. Calvert, H.M. Englund, Handbook of Air Pollution Technology, first ed., John Wiley & Sons, New York, 1984.
[7] C.M. Leung, C.L. Foo, Ann. Acad. Med. Singap. 21 (1992) 624–629.
[8] S. Park, S.Y. Jin, J. Colloid Interface Sci. 286 (2005) 417–419.
[9] Ch.Y. Wu, Y.I. Chou, S.M. Lai, ECS Trans. 16 (2008) 375–378.
[10] R.A. Michaels, Environ. Health Perspect. 107 (1999) 617–627.
[11] C.E. Amshel, M.H. Fealk, B.J. Phillips, D.M. Caruso, Burns 26 (2000) 493–497.
[12] NEC Direcctive Status Report 2013 Online, http://www.eea.europa.eu/publications/nec-directive-status-report-2013 (accessed January 2015).
[13] N.J. Kim, M. Hirai, M. Shoda, J. Hazard. Mater. 72 (2000) 77–90.
[14] F. Schüth, R. Palkovits, R. Schlögl, D.S. Su, Energy Environ. Sci. 5 (2012) 6278–6289.
[15] Y.C. Chung, C. Huang, C.H. Liu, H. Bai, J. Air Waste Manag. Assoc. 51 (2001) 163–172.

[16] T.L. Huang, K.R. Cliffe, J.M. Macinnes, Environ. Sci. Technol. 34 (2000) 4804–4809.
[17] C.H. Hsu, H. Chu, C.M. Cho, J. Air Waste Manag. Assoc. 53 (2003) 246–252.
[18] C.L. Mangun, R.D. Braatz, J. Economy, A.J. Hall, Ind. Eng. Chem. Res. 28 (1999) 3499–3504.
[19] M.A. Wójtowicz, F.P. Miknis, R.W. Grimes, W.W. Smith, M.A. Serio, J. Hazard. Mater. 74 (2000) 81–89.
[20] A.H. Muenter, B.G. Koehler, J. Phys. Chem. A 104 (2000) 8527–8534.
[21] R. Burch, B.W.L. Southward, J. Catal. 198 (2001) 286–295.
[22] B. Dou, M. Zhang, J. Gao, W. Shen, Ind. Eng. Chem. Res. 41 (2002) 4195–4200.
[23] T. Hasegawa, M. Sato, Combust. Flame 114 (1998) 246–258.
[24] M. Ramírez, J.M. Gómez, G. Aroca, D. Cantero, Chemosphere 74 (2009) 1385–1390.
[25] C.L. Mangun, K.L. Benak, J. Economy, K.L. Foster, Carbon 39 (2001) 1809–1820.
[26] R.E. Critoph, Appl. Therm. Eng. 22 (2002) 667–677.
[27] G. Baquerizo, J.P. Maestre, T. Sakuma, M.A. Deshusses, X. Gamisans, D. Gabriel, J. Lafuente, Chem. Eng. J. 113 (2005) 205–214.
[28] Y.J. Li, J.N. Armor, Appl. Catal. B: Environ. 13 (1997) 131–139.
[29] M.J. Lippits, A.C. Gluhoi, B.E. Nieuwenhuys, Catal. Today 137 (2008) 446–452.
[30] G. Olofsson, A. Hinz, A. Anderson, Chem. Eng. Sci. 59 (2004) 4113–4123.
[31] H.S. Gandhi, M. Shelef, J. Catal. 40 (1975) 312–317.
[32] M. de. Boer, H.M. Huisman, R.J.M. Mos, R.G. Leliveld, A.J. Vandillen, J.W. Geus, Catal. Today 17 (1993) 189–200.
[33] S. Shrestha, M.P. Harold, K. Kamasamudram, A. Yezerets, Top. Catal. 56 (2013) 182–186.
[34] A.Y. Stakheev, D.A. Bokarev, A.I. Mytareva, R.K. Parsapur, P. Selvam, Mendeleev Commun. 24 (2014) 313–315.
[35] R. Burch, B.W.L. Southward, Chem. Commun. 8 (2000) 703–704.
[36] L.I. Darvell, K. Heiskanen, J.M. Jones, A.B. Ross, P. Simell, A. Williams, Catal. Today 81 (2003) 681–692.
[37] R. Burch, B.W.L. Southward, Chem. Commun. 13 (2000) 1115–1116.
[38] R. Burch, B.W.L. Southward, J. Catal. 195 (2000) 217–226.
[39] K. Kamasamudram, A. Yezerets, X. Chen, N.M. Castagnola, H.Y. Chen, SAE Technical Paper 2011-01-1314.
[40] G. Busca, L. Lietti, G. Ramis, F. Berti, Appl. Catal. B: Environ. 18 (1998) 1–36.
[41] M. Radojevic, Environ. Pollut. 102 (1998) 685–689.
[42] P. Forzatti, Appl. Catal. A: Gen. 222 (2001) 221–236.
[43] F. Nakahjima, I. Hamada, Catal. Today 29 (1996) 109–115.
[44] H. Bosch, F. Janssen, Catal. Today 2 (1988) 369–532.
[45] L.J. Muzio, G.C. Quartucy, J.E. Cichanowiczy, Int. J. Environ. Pollut. 17 (2002) 4–30.
[46] Air Pollution Control Technology Fact Sheet Online, http://www.epa.gov/ttncatc1/dir1/fscr.pdf (accessed January 2015).
[47] Regulation (EC) no. 595/2009 of the European Parliament and of the Council of 18 June 2009.
[48] R.Y. Minkara, US Patent 7780 934 B2, 2010.
[49] R.T. Wilburn, T.L. Wright, Power Plant Chem. 6 (2004) 295–304.
[50] L. Larrimore, Div. Fuel Chem. Prepr. 47 (2002) 832–833.
[51] M. Amblard, R. Burch, B.W.L. Southward, Appl. Catal. B: Environ. 22 (1999) L159–L166.
[52] M. Jabłońska, Selective Ammonia Oxidation into Nitrogen and Water Vapour, first ed., LAP Lambert Academic Publishing, Saarbrücken, 2014.
[53] A. Scheuer, W. Hauptmann, A. Drochner, J. Gieshoff, H. Vogel, M. Votsmeier, Appl. Catal. B: Environ. 111–112 (2012) 445–455.
[54] M.S. Kim, D.W. Lee, S.H. Chung, Y.K. Hong, S.H. Lee, S.H. Oh, I.H. Cho, K.Y. Lee, J. Hazard. Mater. 237–238 (2012) 153–160.
[55] P. Forzatti, L. Lietti, E. Tronconi, Nitrogen oxides removal—industrial, in: Encyclopedia of Catalysis, first ed., John Wiley & Sons, New York, 2002.
[56] A. Beretta, N. Usberti, L. Lietti, M. Di Blasi, A. Morandi, C. La Marca, Chem. Eng. J. 257 (2014) 170–183.
[57] R.H. Heck, R.J. Farrauto, S.T. Gulati, Catalytic Air Pollution Control: Commercial Technology, second ed., John Wiley & Sons, New York, 2002.
[58] E.S. Gil, Evaluation of ammonia slip catalysts, in: Master's Thesis in the Master's Programme Innovative and Sustainable Chemical Engineering, Chalmers University of Technology, 2013.
[59] J. Balland, M. Parmentier, J. Schmitt, SAE Technical Paper 2014-01-1522.
[60] M. Eichelbauma, R.J. Farrautoa, M.J. Castaldia, Appl. Catal. B: Environ. 97 (2010) 90–97.
[61] L. Mussmann, I. Lappas, A. Geisselmann, W. Mueller, US Patent 8695 329 B2, 2014.
[62] D.B. Brown, R. Mital, K.A. Jaffri, K.B. Fuqua, US Patent 7908 845 B2, 2011.
[63] T. Minami, I.M. Limited, US Patent 6823 660 B2, 2004.
[64] E.V. Gonze, M.J. Paratore, US Patent 8745 970 B2, 2014.
[65] I. Nova, E. Tronconi, Urea-SCR Technology for deNO$_x$ After Treatment of Diesel Exhausts, first ed., Springer, New York, 2014.
[66] N.I. Il'chenko, Russ. Chem. Rev. 45 (1976) 1119–1134.
[67] J.E. Germain, R. Perez, Bull. Soc. Chim. Fr. 5 (1972) 2042–2047.
[68] K. Schmidt-Szałowski, K. Krawczyk, J. Petryk, Appl. Catal. A: Gen. 175 (1998) 147–157.
[69] J. Petryk, E. Kołakowska, Appl. Catal. B: Environ. 24 (2000) 121–128.
[70] G. Olofsson, L.R. Wallenberg, A. Andersson, J. Catal. 230 (2005) 1–13.
[71] J.L. Gong, R.A. Ojifinni, T.S. Kim, J.M. White, C.B. Mullins, J. Am. Chem. Soc. 128 (2006) 9012–9013.
[72] L. Zhang, C.B. Zhang, H. He, J. Catal. 261 (2009) 101–109.
[73] P.D. Sobczyk, E.J.M. Hensen, A.M. de Jong, A.S. van Santen, Top. Catal. 23 (2003) 109–117.
[74] R.Q. Long, R.T. Yang, Catal. Lett. 78 (2002) 353–357.
[75] L. Gang, B.G. Anderson, J. van Grondelle, R.A. van Santen, W.J.H. van Gennip, J.W. Niemantsverdriet, P.J. Kooyman, A. Knoester, H.H. Brongersma, J. Catal. 206 (2002) 60–70.
[76] S.D. Lin, A.C. Gluhoi, B.E. Nieuwenhuys, Catal. Today 90 (2004) 3–14.
[77] J.J. Ostermaier, J.R. Katzer, W.H. Manogue, J. Catal. 33 (1974) 457–473.
[78] L. Gang, B.G. Anderson, J. van Grondelle, R.A. van Santen, Appl. Catal. B: Environ. 40 (2003) 101–110.
[79] A. Scheuer, M. Votsmeier, A. Schuler, J. Gieshoff, A. Drochner, H. Vogel, Top. Catal. 52 (2009) 1847–1851.
[80] J.J. Ostermaier, J.R. Katzer, W.H. Manoque, J. Catal. 41 (1976) 277–292.
[81] L.S. Escandón, S. Ordóñez, F.V. Díez, H. Sastre, React. Kinet. Catal. Lett. 76 (2002) 61–68.
[82] G.I. Golodets, Heterogeneous Catalytic Reactions Involving Molecular Oxygen, first ed., Elsevier, New York, 1983.
[83] R.Q. Long, R.T. Yang, J. Catal. 201 (2001) 145–152.
[84] R.Q. Long, R.T. Yang, J. Catal. 207 (2002) 158–165.
[85] P. Fabrizioli, T. Bürgi, A. Baiker, J. Catal. 206 (2002) 143–154.
[86] A. Wöllner, E. Lange, H. Knozinger, Appl. Catal. A: Gen. 94 (1993) 181–203.
[87] T. Curtin, F. O'Regan, C. Deconinck, N. Knutte, B.H. Hodnett, Catal. Today 55 (2000) 189–195.
[88] L. Lietti, G. Ramirez, G. Busca, F. Bregani, P. Forzatti, Catal. Today 61 (2000) 187–195.
[89] N.N. Sazonova, A.V. Simakov, T.A. Nikoro, G.B. Barannik, V.F. Lyakhova, V.I. Zheivot, Z.R. Ismagilov, H. Veringa, React. Kinet. Catal. Lett. 57 (1996) 71–79.
[90] L. Gang, B.G. Anderson, J. van Grondelle, R.A. van Santen, Catal. Today 61 (2000) 179–185.
[91] J.J.P. Biermann, F.J.J.G. Janssen, J.W. Geus, J. Mol. Catal. 60 (1990) 229–238.
[92] S. Nassos, E. Elm Svensson, M. Nilsson, M. Boutonnet, S. Järås, Appl. Catal. B: Environ. 64 (2006) 96–102.
[93] M. Amblard, R. Burch, B.W.L. Southward, Catal. Today 59 (2000) 365–371.
[94] G. Ramis, M. Angeles Larrubia, J. Mol. Catal. A: Chem. 215 (2004) 161–167.
[95] O.N. Sil'chenkova, V.N. Korchak, V.A. Matyshak, Kinet. Catal. 43 (2002) 363–371.
[96] G. Ramis, L. Yi, G. Busca, Catal. Today 28 (1996) 373–380.
[97] Z. Wang, Z. Qu, X. Quan, Z. Li, H. Wang, R. Fan, Appl. Catal. B: Environ. 134–135 (2013) 153–166.
[98] Ch.M. Hung, Powder Technol. 196 (2009) 56–61.
[99] K. Duan, X. Tang, H. Yi, P. Ning, L. Wang, J. Rare Earths 28 (2010) 338–342.
[100] Z. Wang, Z. Qu, X. Quan, H. Wang, Appl. Catal. A: Gen. 411–412 (2012) 131–138.
[101] J.Ch. Lou, Ch.M. Hung, S.F. Yang, J. Air Waste Manag. Assoc. 54 (2004) 68–76.
[102] L. Zhang, F. Liu, Y. Yu, Y. Liu, Ch. Zhang, H. He, Chin. J. Catal. 32 (2011) 727–735.
[103] L. Gang, J. van Grondelle, B.G. Anderson, R.A. van Santen, J. Catal. 186 (1999) 100–109.
[104] M.S. Kim, D.W. Lee, S.H. Chung, Y.K. Hong, S.H. Lee, S.H. Oh, I.H. Cho, K.Y. Lee, J. Hazard. Mater. 237–238 (2012) 153–160.
[105] R.Q. Long, R.T. Yang, Chem. Commun. 16 (2000) 1651–1652.
[106] M. Jabłońska, A. Król, E. Kukulska-Zając, K. Tarach, L. Chmielarz, K. Góra-Marek, J. Catal. 316 (2014) 36–46.
[107] T. Curtin, S. Lenihan, Chem. Commun. 11 (2003) 1280–1281.
[108] A. Akah, C. Cundy, A. Garforth, Appl. Catal. B: Environ. 59 (2005) 221–226.
[109] A. Akah, G. Nkeng, A. Garforth, Appl. Catal. B: Environ. 74 (2007) 34–39.
[110] G. Qi, Ralph T. Yang, Appl. Catal. A: Gen. 287 (2005) 25–33.
[111] G. Qi, J.E. Gatt, R.T. Yang, J. Catal. 226 (2004) 120–128.
[112] P. Boroń, L. Chmielarz, J. Gurgul, K. Łątka, B. Gil, J.M. Krafft, S. Dzwigaj, Catal. Today 235 (2014) 210–225.
[113] R.W. Mayer, M. Hävecker, A. Knop-Gericke, R. Schlögl, Catal. Lett. 74 (2001) 115–119.
[114] Ch.M. Hung, J. Hazard. Mater. 180 (2010) 561–565.
[115] C.J. Weststrate, J.W. Bakker, A.C. Gluhoi, W. Ludwig, B.E. Nieuwenhuys, Catal. Today 154 (2010) 46–52.
[116] M. Ueshima, K. Sano, M. Ikeda, K. Yoshino, J. Okamura, Res. Chem. Intermediat. 24 (1998) 133–141.
[117] R.W. Mayer, M. Melzer, M. Hävecker, A. Knop-Gericke, J. Urban, H.J. Freund, R. Schlögl, Catal. Lett. 86 (2003) 245–250.
[118] S. Lenihan, T. Curtin, Catal. Today 145 (2009) 85–89.
[119] H.M.J. Kušar, A.G. Ersson, M. Vosecký, S.G. Järås, Appl. Catal. B: Environ. 58 (2005) 25–32.
[120] S. He, Ch. Zhang, M. Yang, Y. Zhang, W. Xu, N. Cao, H. He, Sep. Purif. Technol. 58 (2007) 173–178.
[121] W. Yue, R. Zhang, N. Liu, B. Chen, Chin. Sci. Bull. 59 (2014) 3980–3986.
[122] L. Chmielarz, A. Wegrzyn, M. Wojciechowska, S. Witkowski, M. Michalik, Catal. Lett. 141 (2011) 1345–1354.
[123] L. Chmielarz, M. Jabłońska, A. Strumiński, Z. Piwowarska, A. Węgrzyn, S. Witkowski, M. Michalik, Appl. Catal. B: Environ. 130–131 (2013) 152–162.
[124] L. Chmielarz, P. Kuśtrowski, Z. Piwowarska, M. Michalik, B. Dudek, R. Dziembaj, Top. Catal. 52 (2009) 1017–1022.
[125] L. Chmielarz, P. Kuśtrowski, M. Drozdek, R. Dziembaj, P. Cool, E.F. Vansant, Catal. Today 114 (2006) 319–325.
[126] M.T. Caudle, M. Dieterle, S.E. Buzby, US Patent 0111 796 A1, 2010.
[127] J.M. Jones, M. Pourkashanian, A. Williams, R.I. Backreedy, L.I. Darvell, P. Simell, K. Heiskanen, P. Kilpinen, Appl. Catal. B: Environ. 60 (2005) 139–146.

[128] M. Yang, C. Wu, C. Zhang, H. He, Catal. Today 90 (2004) 263–267.
[129] W. Wang, X. Tang, H. Yi, J. Hu, Adv. Mater. Res. 798–799 (2013) 239–244.
[130] G. Bagnasco, G. Peluso, G. Russo, M. Turco, G. Busca, G. Ramis, Stud. Surf. Sci. Catal. 110 (1997) 643–652.
[131] Ch. Liang, X. Li, Z. Qu, M. Tade, S. Liu, Appl. Surf. Sci. 258 (2012) 3738–3743.
[132] David M. Chapman, Appl. Catal. A: Gen. 392 (2011) 143–150.
[133] J. Engweiler, A. Baiker, Appl. Catal. A: Gen. 120 (1994) 187–205.
[134] K. Bourikas, Ch. Fountzoula, Ch. Kordulis, Appl. Catal. B: Environ. 52 (2004) 145–153.
[135] A. Kaddouri, N. Dupont, P. Gélin, A. Auroux, Catal. Commun. 15 (2011) 32–36.
[136] M. Costa, C.B. Klein, Crit. Rev. Toxicol. 36 (2006) 155–163.
[137] R.B. Hayes, Cancer Causes Control 8 (1997) 371–385.
[138] X. Cui, J. Zhou, Z. Ye, H. Chen, L. Li, M. Ruan, J. Shi, J. Catal. 270 (2010) 310–317.
[139] Ch. M. Hung, Aerosol Air Qual. Res. 6 (2006) 150–169.
[140] J.R. Kim, W.J. Myeong, S.K. Ihm, J. Catal. 263 (2009) 123–133.
[141] G. Avgouropoulos, T. Ioannides, H. Matralis, Appl. Catal. B: Environ. 56 (2005) 87–93.
[142] S. Song, S. Jiang, Appl. Catal. B: Environ. 117–118 (2012) 346–350.
[143] W.B. Williamson, D.R. Flentge, J.H. Lunsford, J. Catal. 37 (1975) 258–266.
[144] L. Chmielarz, P. Kuśtrowski, A. Rafalska-Łasocha, R. Dziembaj, Appl. Catal. B: Environ. 58 (2005) 235–244.
[145] D. Lison, Crit. Rev. Toxicol. 26 (1996) 585–616.
[146] M. Trombetta, G. Ramis, G. Busca, B. Montanari, A. Vaccari, Langmuir 13 (1997) 4628–4637.
[147] M. Jabłońska, L. Chmielarz, A. Węgrzyn, K. Guzik, Z. Piwowarska, S. Witkowski, R.I. Walton, P.W. Dunne, F. Kovanda, J. Therm. Anal. Calorim. 114 (2013) 731–747.
[148] M.T. Caudle, M. Deiterle, S.A. Roth, W-M. Xue, US Patent 7722 845 B2, 2010.
[149] M. Jabłońska, L. Chmielarz, A. Węgrzyn, Chemik 67 (2013) 706–710.
[150] R. Kraehnert, M. Baerns, Chem. Eng. J. 137 (2008) 361–375.
[151] E.V. Rebrov, M.H.J.M. de Croon, J.C. Schouten, Chem. Eng. J. 90 (2002) 61–76.
[152] Z. Zhu, Z. Liu, S. Lin, H. Niu, T. Hu, T. Liu, Appl. Catal. B: Environ. 26 (2000) 25–35.
[153] G. Centi, C. Nigro, S. Perathoner, G. Stella, Catal. Today 17 (1993) 159–166.
[154] G. Ramis, L. Yi, G. Busca, M. Turco, E. Kotur, R.J. Willey, J. Catal. 157 (1995) 523–535.
[155] F. Dannevang, US Patent 5587 134, 1996.
[156] L. Lietti, G. Groppi, C. Ramella, Catal. Lett. 53 (1998) 91–95.
[157] L. Lietti, C. Cristiani, G. Groppi, P. Forzatti, Catal. Today 59 (2000) 191–204.
[158] M.F.M. Zwinkels, G.M.E. Heginuz, B.H. Gregertsen, K. Sjöström, S.G. Järås, Appl. Catal. A: Gen. 148 (1997) 325–341.
[159] M. Colombo, I. Nova, E. Tronconi, Chem. Eng. Sci. 75 (2012) 75–83.
[160] A. Scheuer, W. Hauptmann, A. Drochner, H. Vogel, J. Gieshoff, M. Votsmeier, Appl. Catal. B: Environ. 111–112 (2010) 445–455.
[161] S. Shrestha, M.P. Harold, K. Kamasamudram, A. Yezerets, AIChE Annual Meeting, November 3–8, 2013, Conference Proceedings, 2013.
[162] M.T. Caudle, M. Deiterle, S.A. Roth, W.M. Xue, US Patent 0292 519 A1, 2008.
[163] M. Colombo, I. Nova, E. Tronconi, V. Schmeiβer, B. Bandl-Konrad, L. Zimmermann, Appl. Catal. B: Environ. 142–143 (2013) 861–876.
[164] R. Nedyalkova, K. Kamasamudram, N.W. Currier, J. Li, A. Yezerets, J. Catal. 299 (2013) 101–108.
[165] K. Kamasamudram, N.W. Currier, X. Chen, A. Yezerets, Catal. Today 151 (2010) 212–222.
[166] N. Wilken, K. Kamasamudram, N.W. Currier, J. Li, A. Yezerets, L. Olsson, Catal. Today 151 (2010) 237–243.
[167] X. Auvray, W.P. Partridge, J.S. Choi, J.A. Pihl, A. Yezerets, K. Kamasamudram, N.W. Currier, L. Olsson, Appl. Catal. B: Environ. 126 (2012) 144–152.
[168] H. Sjövall, L. Olsson, E. Fridell, R.J. Blint, Appl. Catal. B: Environ. 64 (2006) 180–188.
[169] H.W. Nasution, E. Purnama, S. Kosela, J. Gunlazuardi, Catal. Commun. 6 (2005) 313–319.
[170] F.E. López-Suárez, A. Bueno-López, M.J. Illán-Gómez, Appl. Catal. B: Environ. 84 (2008) 651–658.
[171] N.I. Il'chenko, G.I. Golodets, J. Catal. 39 (1976) 57–72.
[172] G.J. Golodets, Y.I. Pyatnitskii, Kinet. Katal. 4 (1968) 25–40.
[173] E.M. Slavinskaya, S.A. Veniaminov, P. Notté, A.S. Ivanova, A.I. Boronin, Y.A. Chesalov, I.A. Polukhina, A.S. Noskov, J. Catal. 222 (2004) 129–142.
[174] L. Chmielarz, P. Kuśtrowski, A. Rafalska-Łasocha, D. Majda, R. Dziembaj, Appl. Catal. B: Environ. 35 (2002) 195–210.
[175] S.K. Kim, K.H. Kim, S.K. Ihm, Chemosphere 68 (2007) 287–292.
[176] K.V.R. Chary, K.K. Seela, D.N.P. Ramakanth, Catal. Commun. 9 (2008) 75–81.
[177] W.P. Dow, Y.P. Wang, T.J. Huang, Appl. Catal. A: Gen. 190 (2000) 25–34.
[178] N.I. Il'chenko, G.I. Golodets, J. Catal. 39 (1975) 73–86.
[179] R. Burch, B.W.L. Southward, Chem. Commun. 16 (1999) 1475–1476.
[180] L. Chmielarz, P. Kuśtrowski, R. Dziembaj, P. Cool, E.F. Vansant, Appl. Catal. B: Environ. 62 (2006) 369–380.
[181] J.M.G. Amores, V. Sanchez Escribano, G. Ramis, G. Busca, Appl. Catal. B: Environ. 13 (1997) 45–58.
[182] N.Y. Topsøe, Science 265 (1994) 1217–1219.
[183] N.Y. Topsøe, H. Topsøe, J.A. Dumesic, J. Catal. 151 (1995) 226–240.
[184] N.Y. Topsøe, H. Topsøe, J.A. Dumesic, J. Catal. 151 (1995) 241–252.
[185] R.M. Yuan, G. Fu, X. Xu, H.L. Wan, J. Phys. Chem. C 115 (2011) 21218–21229.
[186] Ch.M. Hung, Powder Technol. 200 (2010) 78–83.
[187] J. Leppälahti, T. Koljonen, M. Hupa, P. Kilpinen, Energy Fuels 11 (1997) 30–38.
[188] Self-Study Programme 230: Motor Vehicle Exhaust Emissions Online, www.volkspage.net/technik/ssp/ssp/SSP_230.pdf, (accessed January 2015).
[189] S.M. Jeong, S.H. Jung, K.S. Yoo, S.D. Kim, Ind. Eng. Chem. Res. 38 (1999) 2210–2215.
[190] J. Zawadzki, Discuss. Faraday Soc. 8 (1950) 140–152.
[191] M. Amblard, R. Burch, B.W.L. Southward, Catal. Lett. 68 (2000) 105–108.
[192] L. Chmielarz, P. Kuśtrowski, M. Michalik, B. Dudek, Z. Piwowarska, R. Dziembaj, Catal. Today 137 (2008) 242–246.
[193] E. Brocławik, J. Datka, B. Gil, P. Kozyra, Catal. Today 75 (2002) 353–357.
[194] L. Chmielarz, A. Kowalczyk, M. Wojciechowska, P. Boroń, B. Dudek, M. Michalik, Chem. Pap. 68 (2014) 1219–1227.
[195] B. Montanari, A. Vaccari, M. Gazzano, P. Käßner, H. Papp, J. Pasel, R. Dziembaj, W. Makowski, T. Łojewski, Appl. Catal. B: Environ. 16 (1996) 205–217.
[196] L. Chmielarz, Z. Piwowarska, P. Kuśtrowski, A. Węgrzyn, B. Gil, A. Kowalczyk, B. Dudek, R. Dziembaj, M. Michalik, Appl. Clay Sci. 53 (2011) 164–173.
[197] L. Chmielarz, P. Kuśtrowski, A. Rafalska-Łasocha, D. Majda, R. Dziembaj, Appl. Catal. B: Environ. 35 (2002) 195–210.
[198] U. De La Torre, B. Pereda-Ayo, J.R. González-Velasco, Chem. Eng. J. 207–208 (2012) 10–17.
[199] J. Pérez-Ramírez, E.V. Kondratenko, G. Novell-Leruth, J.M. Ricart, J. Catal. 261 (2009) 217–223.
[200] J. Pérez-Ramírez, F. Kaptein, K. Schöffer, J.M. Moulijn, Appl. Catal. B: Environ. 44 (2003) 117–151.
[201] T. Pignet, L.D. Schmidt, J. Catal. 40 (1975) 212–225.
[202] G.S. Selwyn, G.T. Fujimoto, M.C. Lin, J. Phys. Chem. 86 (1982) 760–765.
[203] W.D. Mieher, W. Ho, Surf. Sci. 322 (1995) 151–167.
[204] J. Pérez-Ramírez, E.V. Kondratenko, V.A. Kondratenko, M. Baerns, J. Catal. 229 (2005) 303–313.
[205] T. Katona, L. Guczi, G.A. Somorjai, J. Catal. 135 (1992) 434–443.
[206] T. Katona, G.A. Somorjai, J. Phys. Chem. 96 (1992) 5465–5472.
[207] A.P. Seitsonen, D. Crihan, M. Knapp, A. Resta, E. Lundgren, J.N. Andersen, H. Over, Surf. Sci. 603 (2009) L113–L116.
[208] K. Otto, M. Shelef, J.T. Kummer, J. Phys. Chem. 74 (1970) 2690–2696.
[209] K. Otto, M. Shelef, J.T. Kummer, J. Phys. Chem. 75 (1971) 875–879.